

## Supporting information (SI)

**A simple and efficient strategy for the preparation of insensitive energetic materials: cyclization of picrylhydrazone affords the indazole derivatives**

Jie Tang, Jieyi Chen, Pengju Yang, Hongwei Yang\* and Guangbin Cheng\*

School of Chemical Engineering, Nanjing University of Science and Technology

Nanjing 210094, P. R. China

**Email: [gcheng@mail.njust.edu.cn](mailto:gcheng@mail.njust.edu.cn)**

**[hyang@mail.njust.edu.cn](mailto:hyang@mail.njust.edu.cn)**

---

## Table of Contents

<b>1</b>	<b>Experimental section.....</b>	<b>3</b>
<b>2</b>	<b>The crystallographic data.....</b>	<b>4</b>
<b>3</b>	<b>Theoretical study.....</b>	<b>6</b>
<b>4</b>	<b>Thermal behaviors .....</b>	<b>9</b>
<b>5</b>	<b>Reference.....</b>	<b>12</b>
<b>6</b>	<b><sup>1</sup>H and <sup>13</sup>C NMR spectra of compounds .....</b>	<b>13</b>
<b>7</b>	<b>Mass spectra of compounds.....</b>	<b>24</b>

---

## 1 Experimental section

### General methods

$^1\text{H}$  and  $^{13}\text{C}$  NMR spectra were recorded on 500 MHz (Bruker AVANCE 500) nuclear magnetic resonance spectrometers operating at 500 and 125 MHz, respectively, by using either  $\text{DMSO-}d_6$  or  $\text{acetone-}d_6$  as the solvent and locking solvent unless otherwise stated. Chemical shifts in  $^1\text{H}$  and  $^{13}\text{C}$  NMR spectra are reported relative to DMSO. DSC was performed at a heating rate of  $5\text{ }^\circ\text{C min}^{-1}$  in closed Al containers with a nitrogen flow of  $30\text{ mL min}^{-1}$  on an STD-Q600 instrument. Infrared (IR) spectra were recorded on a Perkin-Elmer Spectrum BX FT-IR equipped with an ATR unit at  $25\text{ }^\circ\text{C}$ . Impact sensitivity, friction sensitivity and electrostatic discharge sensitivity of samples are measured by using the standard BAM methods.

### X-ray crystallography

The data were collected with a Bruker three-circle platform D8 VENTURE with graphite-monochromated  $\text{Mo K}\alpha$  radiation ( $\lambda = 0.71073\text{ \AA}$ ). A Kryo-Flex low-temperature device was used during the data collection. The data collection and the initial unit cell refinement were performed by using APEX2 (v2010.3-0). Data reduction was performed by using SAINT (v7.68A) and XPREP (v2008/2). Corrections were applied for Lorentz, polarization, and absorption effects by using SADABS (v2008/1). The structure was solved and refined with the aid of the programs in the SHELXTL-plus (v2008/4) system of programs. The full-matrix least-squares refinement on  $F^2$  included atomic coordinates and anisotropic thermal parameters for all non-H atoms. The H atoms were included in a riding model. The structure was solved by direct methods with SHELXS-97 and expanded by using the Fourier technique. The nonhydrogen atoms were refined anisotropically. The hydrogen atoms were located and refined.

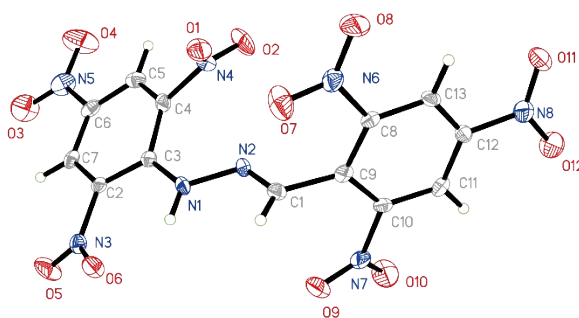
## 2 The crystallographic data

The crystal of **2a**, **4a • DMF** and **5b** were performed on D8 VENTURE with graphite-monochromated Mo K $\alpha$  radiation ( $\lambda = 0.71073$  Å), respectively. Integration and scaling of intensity data were accomplished using the SAINT program. The structures were solved by intrinsic using SHELXT2014 and refinement was carried out by a full-matrix least-squares technique using SHELXT2018. The hydrogen atoms were refined isotropically, and the heavy atoms were refined anisotropically. N-H and O-H hydrogens were located from different electron density maps, and C-H hydrogens were placed in calculated positions and refined with a riding model. Data were corrected for the effects of absorption using SADABS Relevant crystal data and refinement results are summarized in Table S1.

**Table S1.** Crystal data and structure refinement for **2a**, **4a • DMF** and **5b**.

Crystal	<b>2a</b>	<b>4a • DMF</b>	<b>5b</b>
CCDC number	1900161	2011493	2005063
Empirical formula	C <sub>13</sub> H <sub>6</sub> N <sub>8</sub> O <sub>12</sub>	C <sub>22</sub> H <sub>22</sub> N <sub>16</sub> O <sub>14</sub>	C <sub>15</sub> H <sub>8</sub> N <sub>10</sub> O <sub>10</sub>
Formula weight	466.26	734.55	488.31
Temperature	173(2) K	170.0 K	100 K
Crystal system	monoclinic	triclinic	monoclinic
Space group	P21/n	<i>P</i> -1	<i>C</i> 2/ <i>c</i>
<i>a</i> [Å]	8.4477(6) Å	7.8751(4) Å	26.618(10) Å
<i>b</i> [Å]	9.0068(5) Å	8.0958(3) Å	15.497(6) Å
<i>c</i> [Å]	23.0450(17) Å	12.3520(5) Å	9.320(3) Å
$\alpha$ [°]	90°	81.816(2)°	90°
$\beta$ [°]	93.494(3)°	80.771(2)°	97.757(10)°
$\gamma$ [°]	90°	80.036(2)°	90°
Volume	1750.2(2)	760.25(6) Å <sup>3</sup>	3809(2) Å <sup>3</sup>
<i>Z</i>	4	1	8
$\rho$ (g cm <sup>-3</sup> )	1.770	1.604	1.703
F(000)	944.0	378.0	1984.0

Crystal size (mm <sup>3</sup> )	0.32 × 0.16 × 0.04	0.15 × 0.08 × 0.05	0.04 × 0.02 × 0.01
Theta range for data collection	6.62° to 50.752°	5.144° to 52.938°	5.032° to 50.054°
Index ranges	-10 ≤ h ≤ 10, -10 ≤ k ≤ 10, -27 ≤ l ≤ 27	-9 ≤ h ≤ 9, -9 ≤ k ≤ 10, --15 ≤ l ≤ 15	-27 ≤ h ≤ 31, -18 ≤ k ≤ 16, -10 ≤ l ≤ 11
Reflections collected	12208	8624	11573
Independent reflections	3185	3092	3253
Goodness-of-fit on F <sup>2</sup>	1.097	1.051	1.057
Final R indices [I > 2σ(I)]	R <sub>1</sub> = 0.0599, wR <sub>2</sub> = 0.0943	R <sub>1</sub> = 0.0404, wR <sub>2</sub> = 0.0859	R <sub>1</sub> = 0.1084, wR <sub>2</sub> = 0.2653
R indices (all data)	R <sub>1</sub> = 0.1011, wR <sub>2</sub> = 0.1060	R <sub>1</sub> = 0.0650, wR <sub>2</sub> = 0.0983	R <sub>1</sub> = 0.1762, wR <sub>2</sub> = 0.3001



---

Figure S1. The molecule structure of compound **2a** (Thermal ellipsoids represent the 50% probability level.)

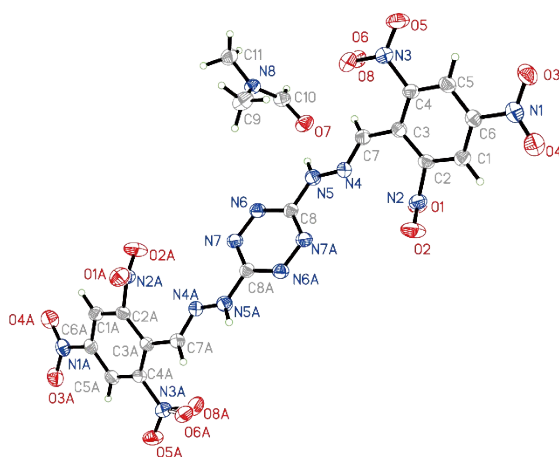


Figure S2. The molecule structure of compound **4a** (Thermal ellipsoids represent the 50% probability level.)

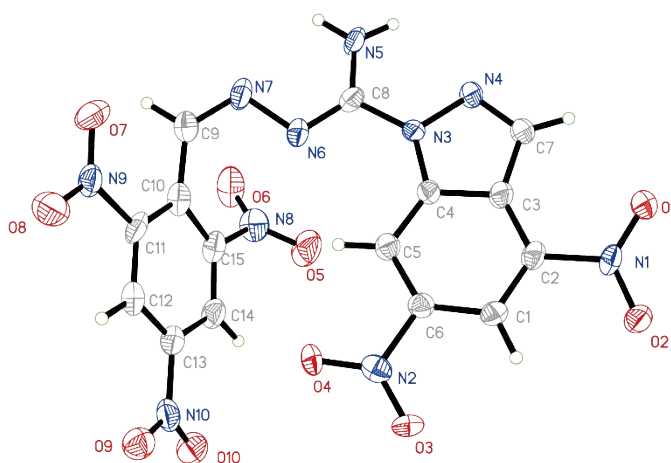


Figure S3. The molecule structure of compound **5b** (Thermal ellipsoids represent the 50% probability level.)

---

### 3 Theoretical study

Theoretical calculations were performed by using the Gaussian 09 (Revision D.01) suite of programs.<sup>[1]</sup> The elementary geometric optimization and the frequency analysis were performed at the level of the Becke three parameter, Lee-Yan-Parr (B3LYP)[9] functional with the 6-311+G\*\* basis set.<sup>[2]</sup> All of the optimized structures were characterized to be local energy minima on the potential surface without any imaginary frequencies. Atomization energies were calculated by the CBS-4M.<sup>[3]</sup> All the optimized structures were characterized to be true local energy minima on the potential-energy surface without imaginary frequencies.<sup>[4]</sup>

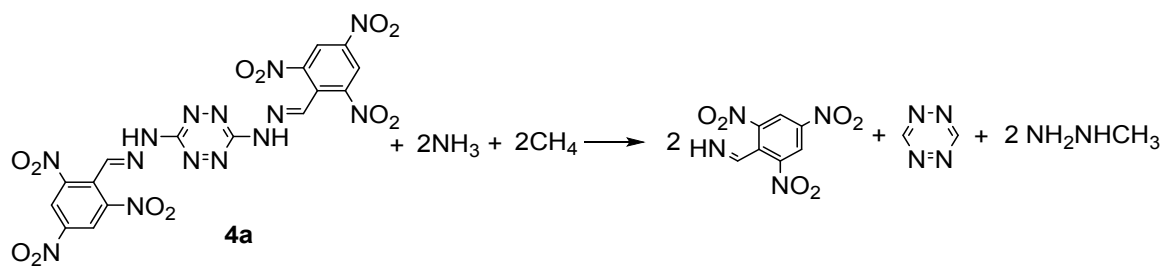
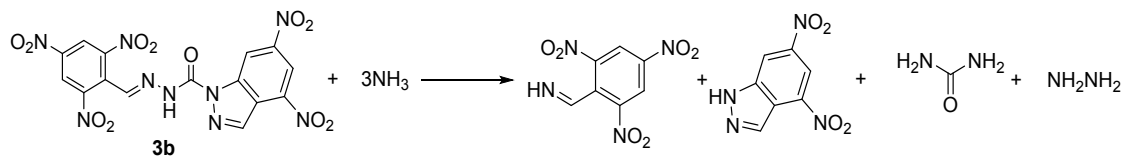
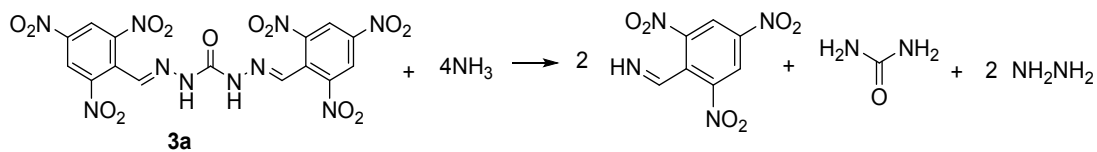
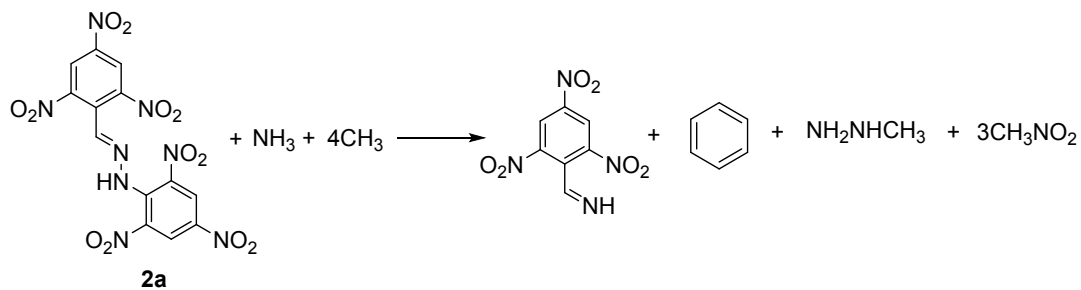
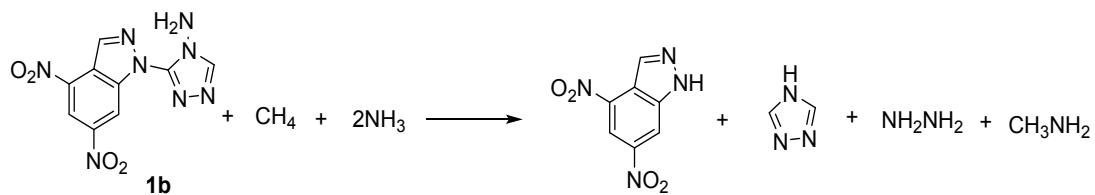
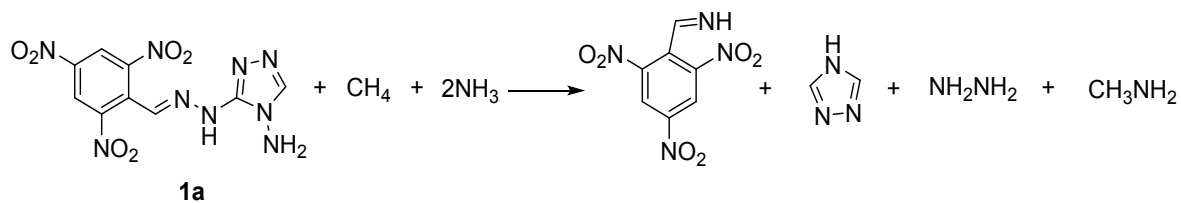
The predictions of heat of formation (*HOF*) adopt the hybrid DFT-B3LYP methods with 6-311+G\*\* basis set via designed isodesmic reactions. The isodesmic reaction processes, i.e., the number of each kind of formal bond is conserved, are used with application of the bond separation reaction (BSR) rules. The molecule is broken down into a set of two heavy-atom molecules containing the same component bonds. The isodesmic reactions used to derive the *HOF* of the title compounds are in Scheme S1. The change of enthalpy for the reactions at 298 K can be expressed as

$$\Delta H_{298} = \sum \Delta_f H_P - \sum \Delta_f H_R \quad (1)$$

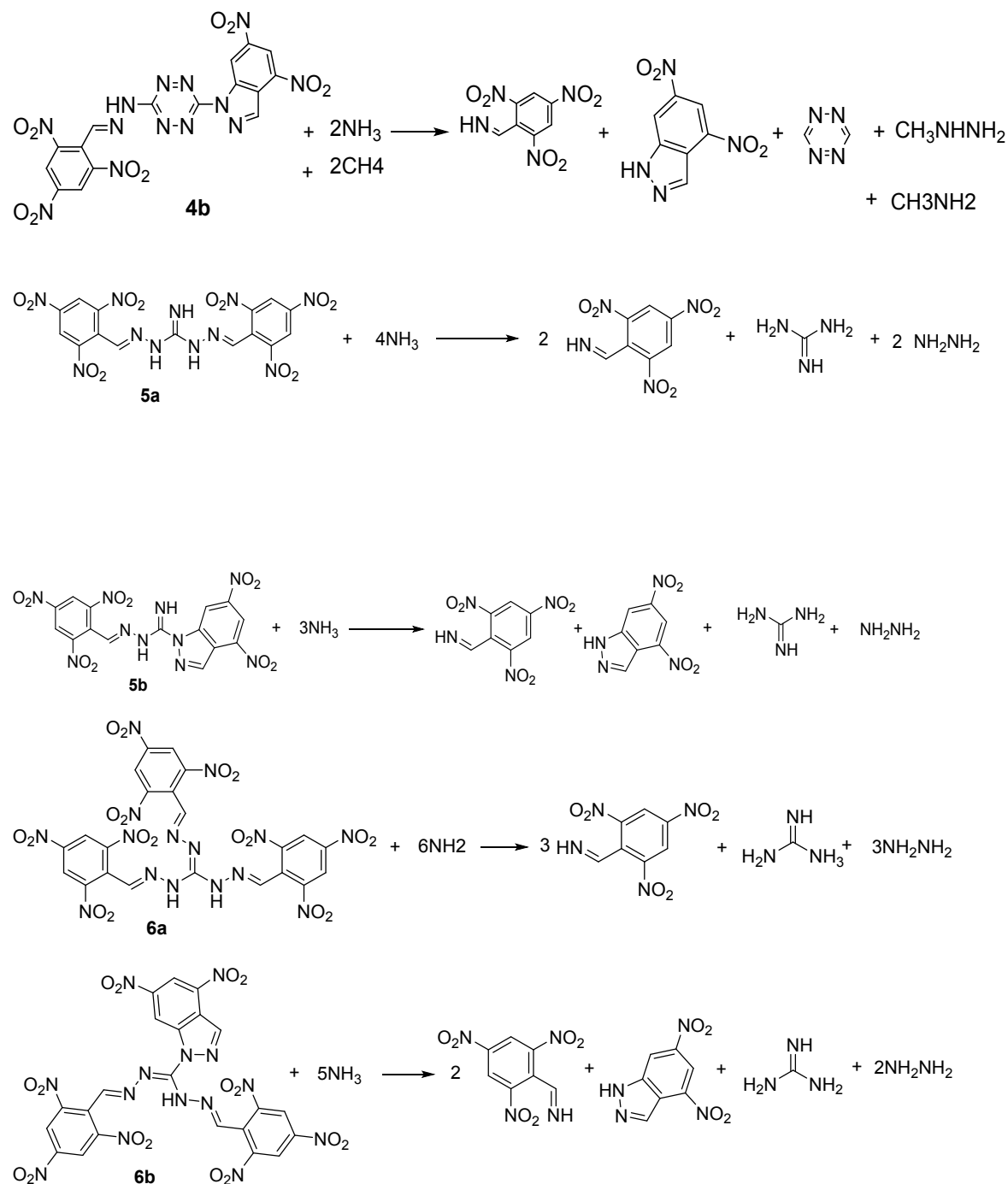
Where  $\sum \Delta_f H_P$  and  $\sum \Delta_f H_R$  are the *HOF* of reactants and products at 298 K, respectively, and  $\Delta H_{298}$  can be calculated using the following expression:

$$\Delta H_{298} = \Delta E_{298} + \Delta(PV) = \Delta E_0 + \Delta ZPE + \Delta H_T + \Delta nRT \quad (2)$$

Where  $\Delta E_0$  is the change in total energy between the products and the reactants at 0 K;  $\Delta ZPE$  is the difference between the zero-point energies (*ZPE*) of the products and the reactants at 0 K;  $\Delta H_T$  is thermal correction from 0 to 298 K. The  $\Delta(PV)$  value in eq (2) is the *PV* work term. It equals  $\Delta(nRT)$  for the reactions of ideal gas. For the isodesmic reaction,  $\Delta n = 0$ , so  $\Delta(PV) = 0$ . On the left side of Eq. (1), apart from target compound, all the others are called reference compounds. The *HOF* of reference compounds is available from the experiments:

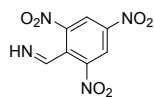


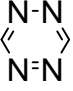
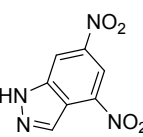
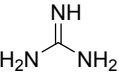
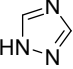




**Scheme S1.** Isodesmic reactions of target compounds.

**Table S2.** Ab initio computational values of small molecules used in isodesmic and tautomeric reactions.

Compound	E <sub>0</sub> <sup>a</sup>	ZPE <sup>b</sup>	H <sub>1</sub> <sup>c</sup>	HOF <sup>d</sup>
NH <sub>2</sub> NH <sub>2</sub>	-111.91	134.28	11.16	95.4
CH <sub>3</sub> NH <sub>2</sub>	-95.89	160.78	11.64	-22.5
	-939.46	322.67	41.27	147.84

	-296.40	128.90	13.87	469.38
	-789.06	307.27	33.26	173.78
	-205.44	184.19	14.19	30.52
	-242.32	150.39	12.06	192.7

<sup>a</sup>Total energy calculated by B3LYP/6-311+G\*\*method (a.u); <sup>b</sup>zero-point correction (kJ mol<sup>-1</sup>); <sup>c</sup> thermal correction to enthalpy (kJ mol<sup>-1</sup>); <sup>d</sup> heat of formation (kJ mol<sup>-1</sup>).

#### 4 Thermal Behaviors

The thermal behavior of compounds **1a-6a**, **1b**, **3b-7b** were investigated by differential scanning calorimetry (DSC) at a heating rate of 5 °C min<sup>-1</sup>.

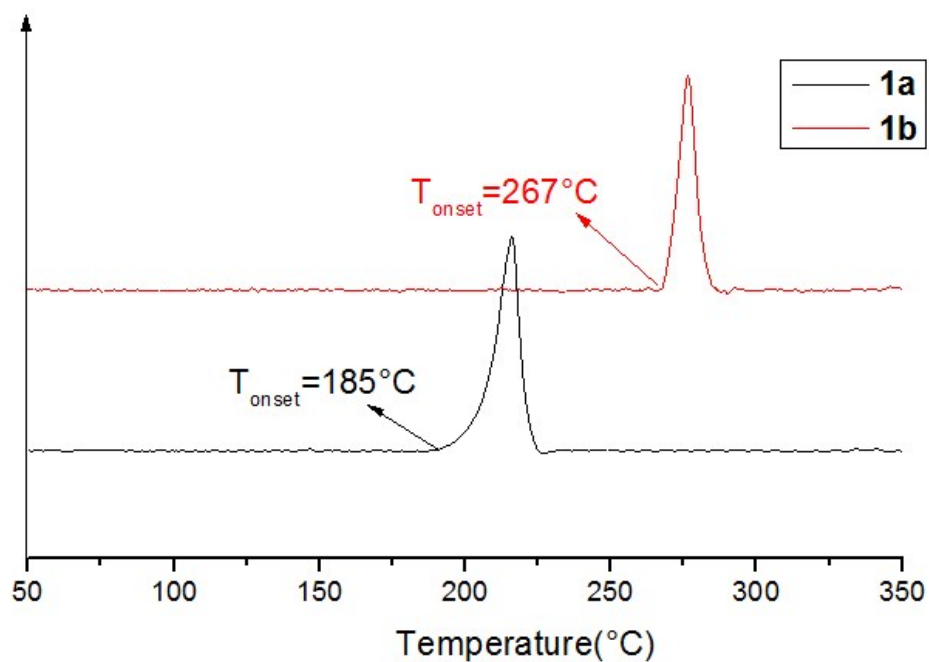


**Figure S4.** DSC plot of **1a** and **1b**.

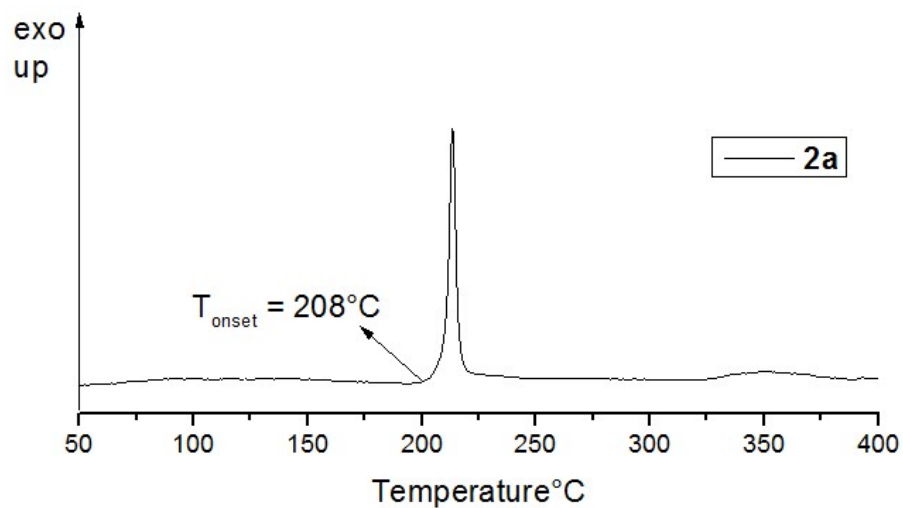


**Figure S5.** DSC plot of 2a.

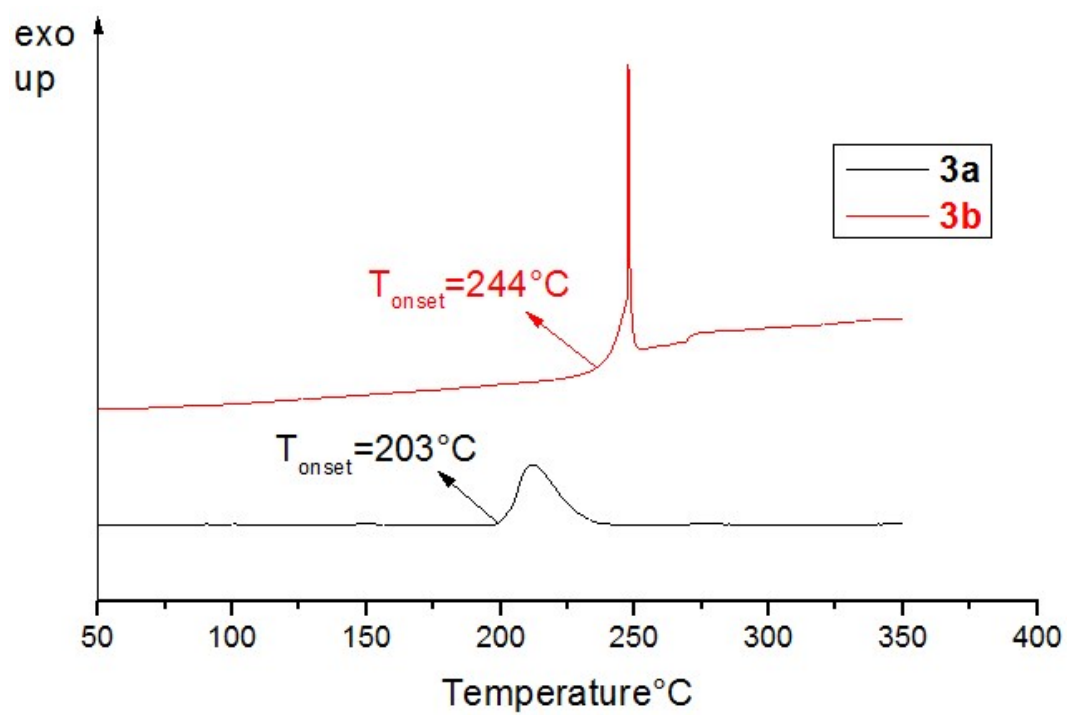


**Figure S6.** DSC plot of 3a and 3b.

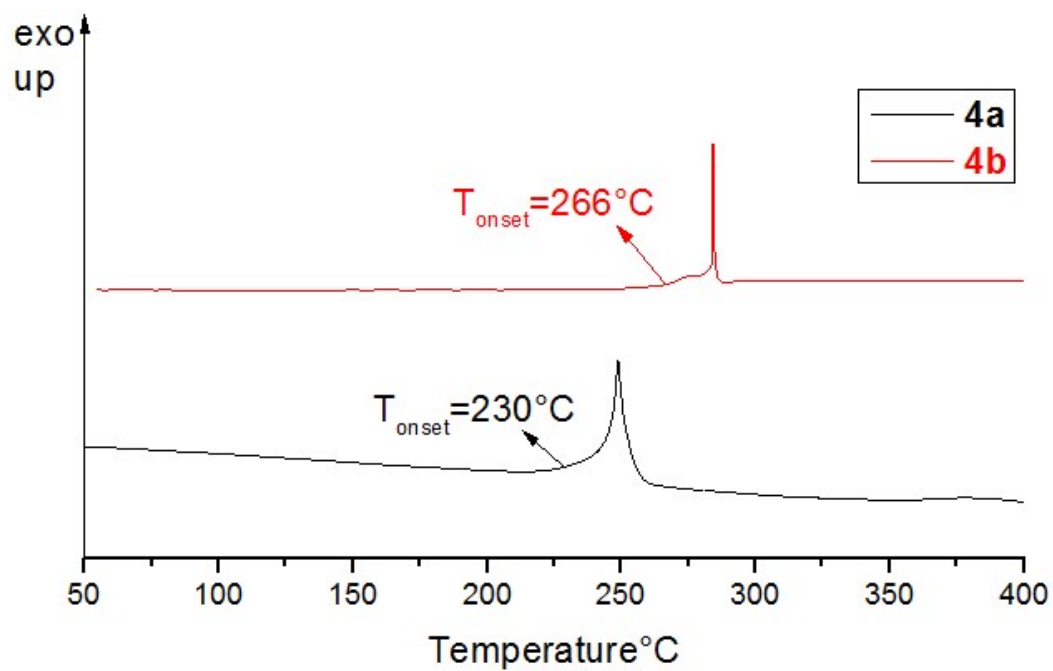


Figure S7. DSC plot of 4a and 4b.

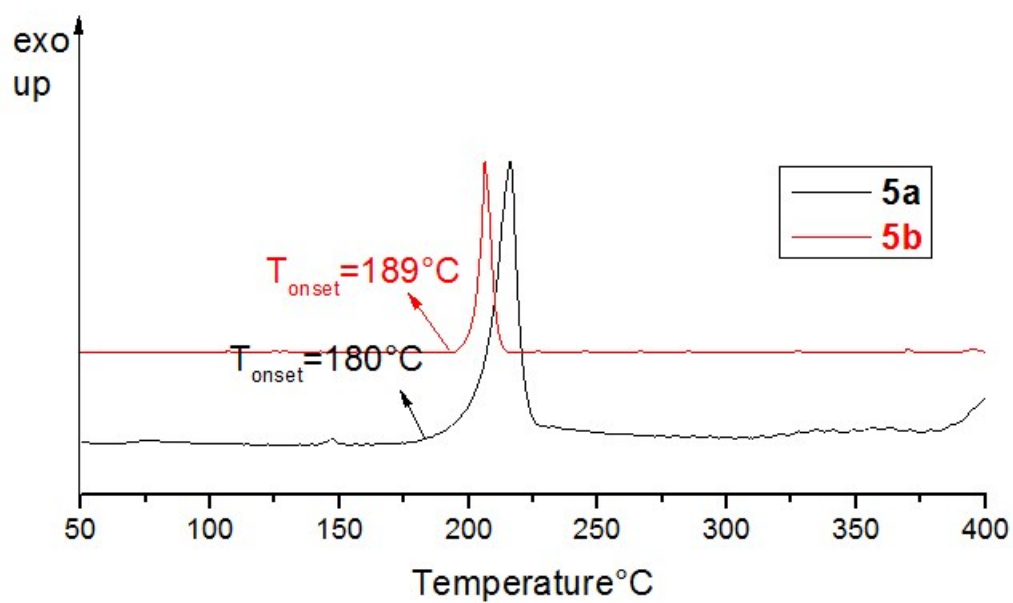
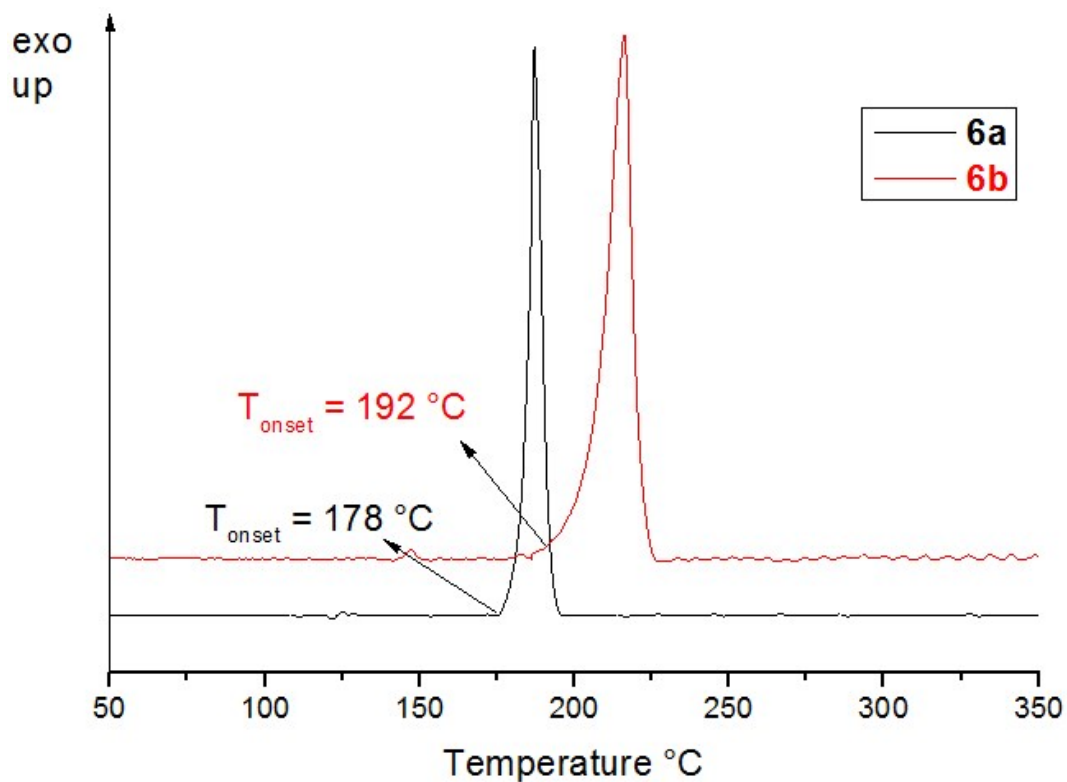


Figure S8. DSC plot of 5a and 5b.



**Figure S9.** DSC plot of **6a** and **6b**.

## 5 Reference

- [1] Frisch, M. J.; Trucks, G. W.; Schlegel, H. B.; Daniels, A. D.; Farkas, O.; Foresman, J. B.; Ortiz, J. V.; Cioslowski, J.; Fox, D. J. Gaussian 09, Revision D. 01, Gaussian, Inc. Wallingford CT, **2009**.
- [2] P. C. Hariharan, J. A. Pople, *Theor. Chim. Acta.* 1973, 28, 213-222.
- [3] J. W. Ochterski, G. A. Petersson, J. A. Montgomery, *J. Chem. Phys.* 1996, 104, 2598-2619.
- [4] H. D. B. Jenkins, D. Tudeal, L. Glasser, *Inorg. Chem.* 2002, 41, 2364-2367.

**6  $^1\text{H}$  and  $^{13}\text{C}$  NMR spectra of compounds**

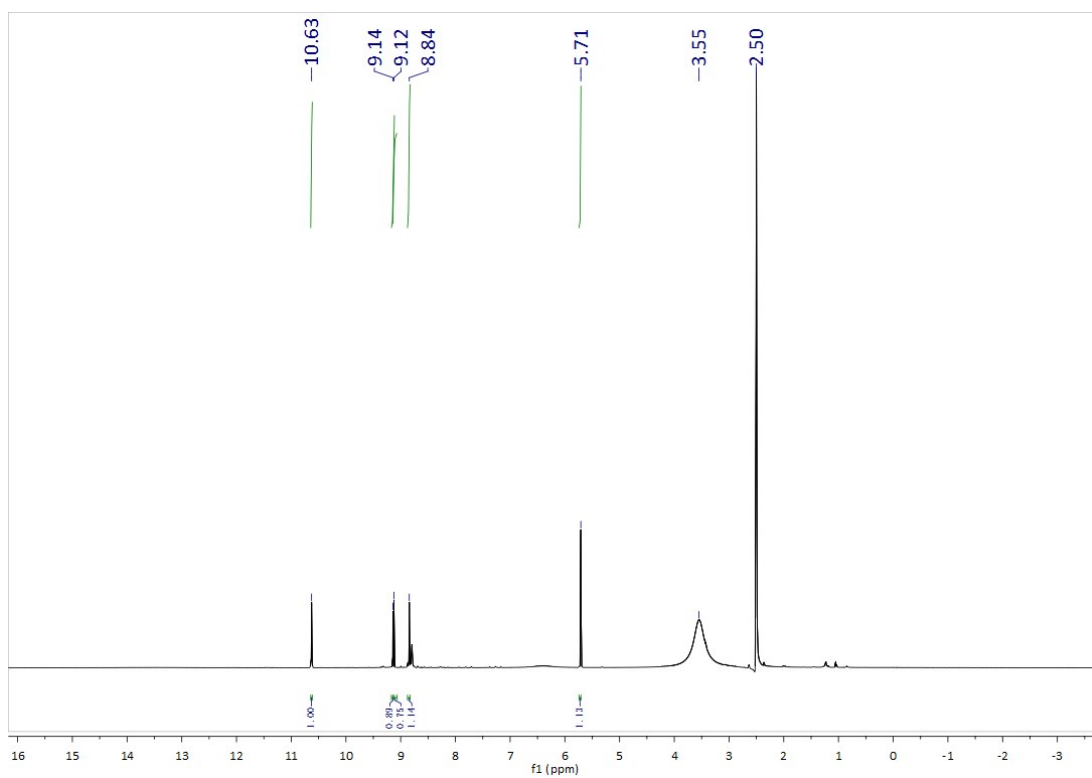


**Figure S10**  $^1\text{H}$  NMR spectra (500 MHz) of **1a** in  $[\text{D}_6]$  DMSO at 25 °C.

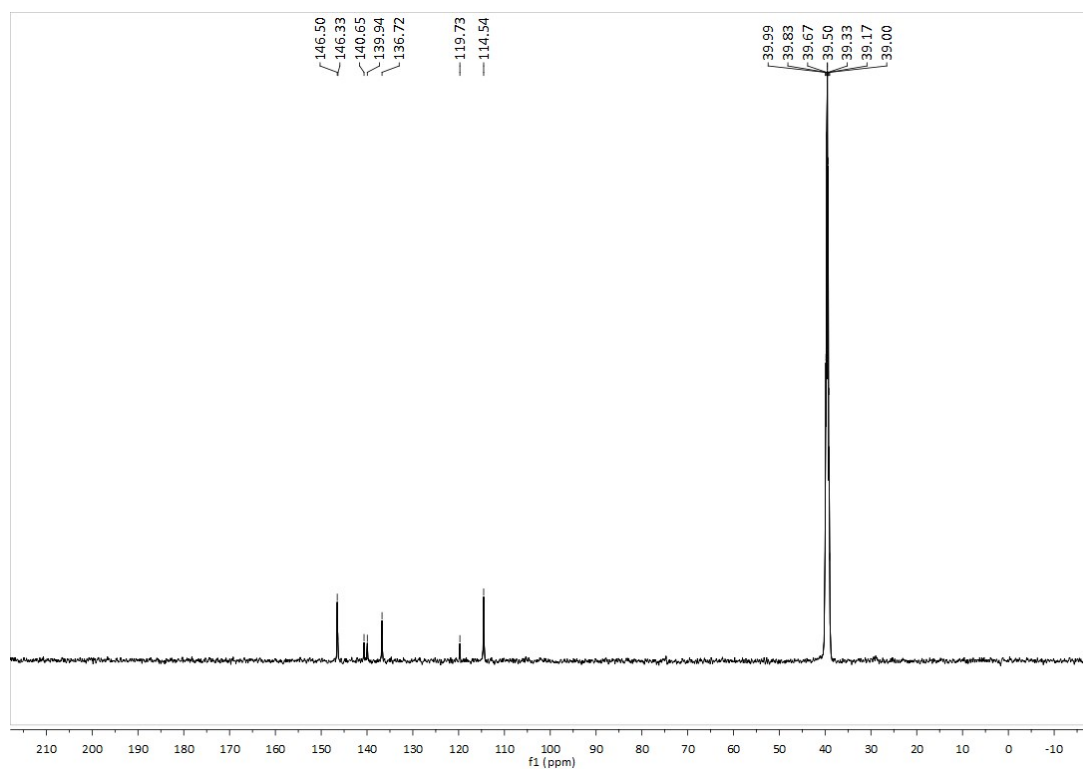


**Figure S11**  $^{13}\text{C}$  NMR spectra (125 MHz) of **1a** in  $[\text{D}_6]$  DMSO at 25 °C.

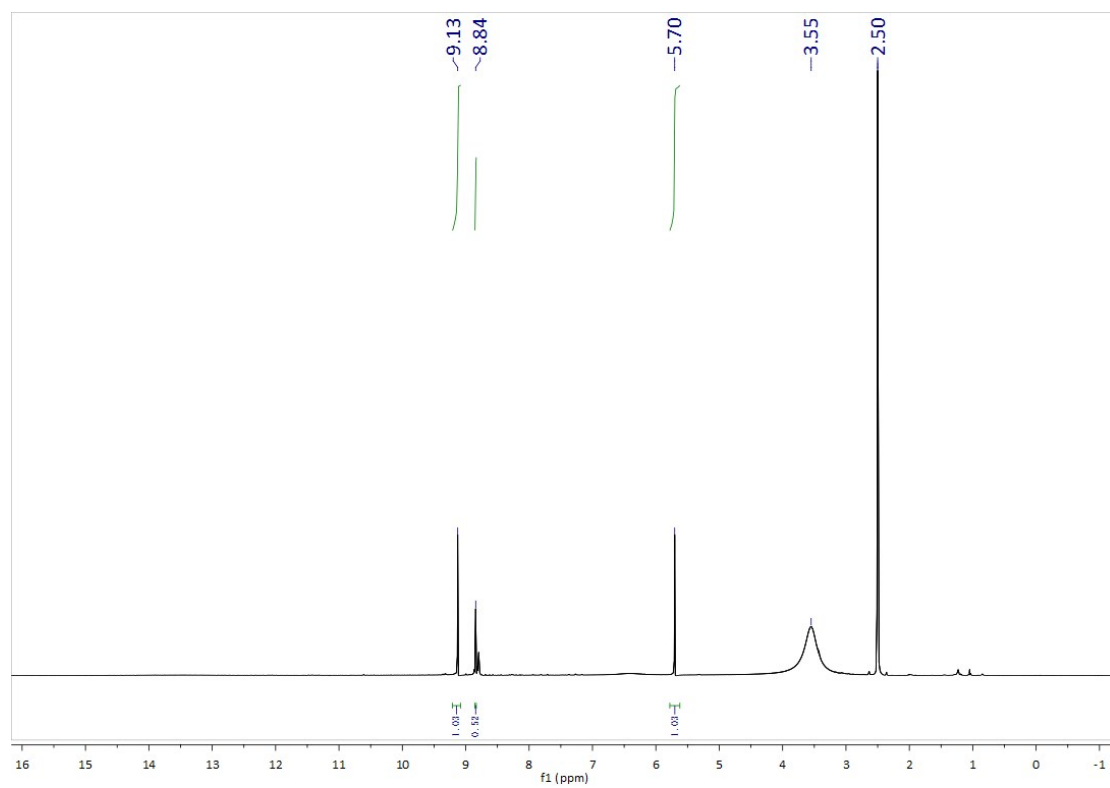


**Figure S12**  $^1\text{H}$  NMR spectra (500 MHz) of **1b** in  $[\text{D}_6]$  DMSO at 25 °C

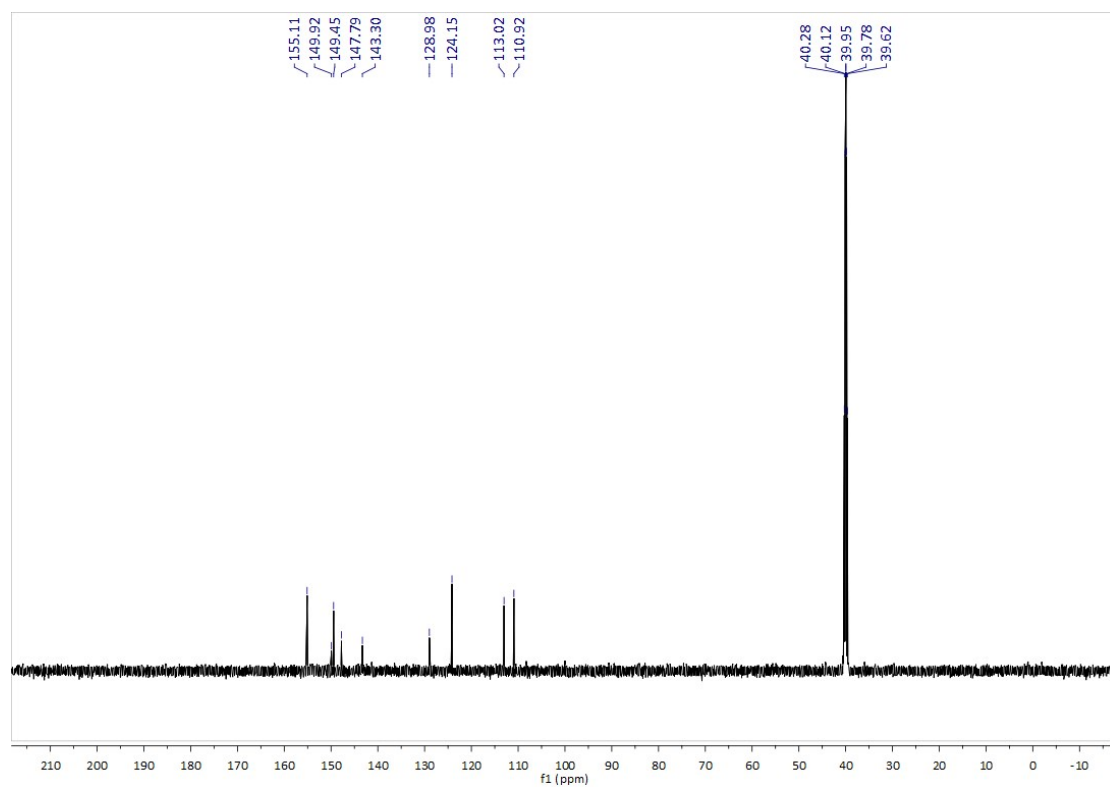


**Figure S13** <sup>13</sup>C NMR spectra (125 MHz) of **1b** in [D<sub>6</sub>] DMSO at 25 °C

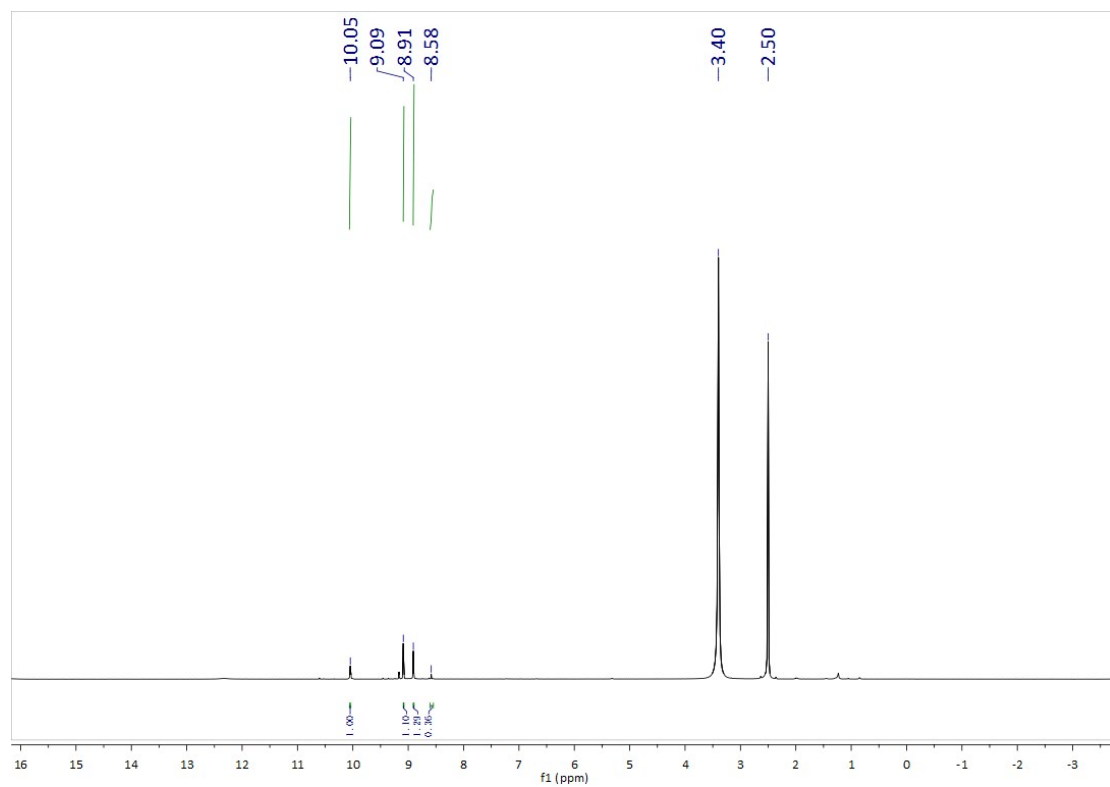


**Figure S14** <sup>1</sup>H NMR spectra (500 MHz) of **2a** in [D<sub>6</sub>] DMSO at 25 °C



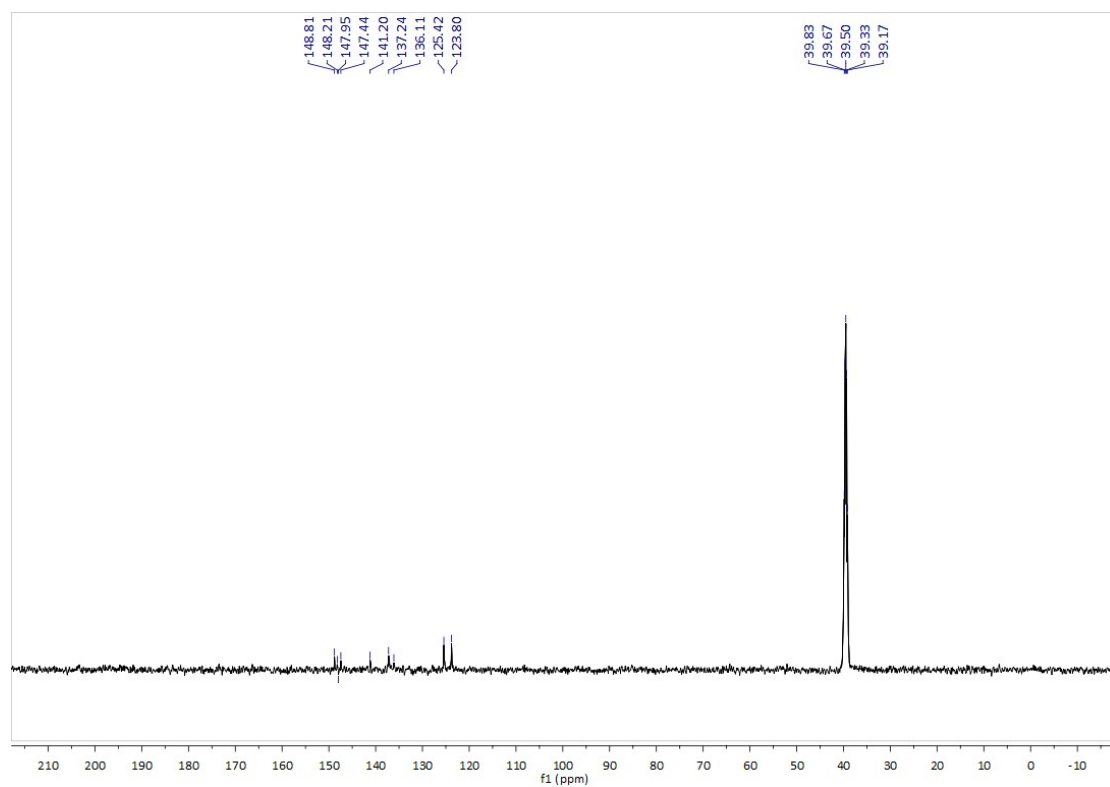


**Figure S15**  $^{13}\text{C}$  NMR spectra (125 MHz) of **2a** in  $[\text{D}_6]$  DMSO at 25 °C

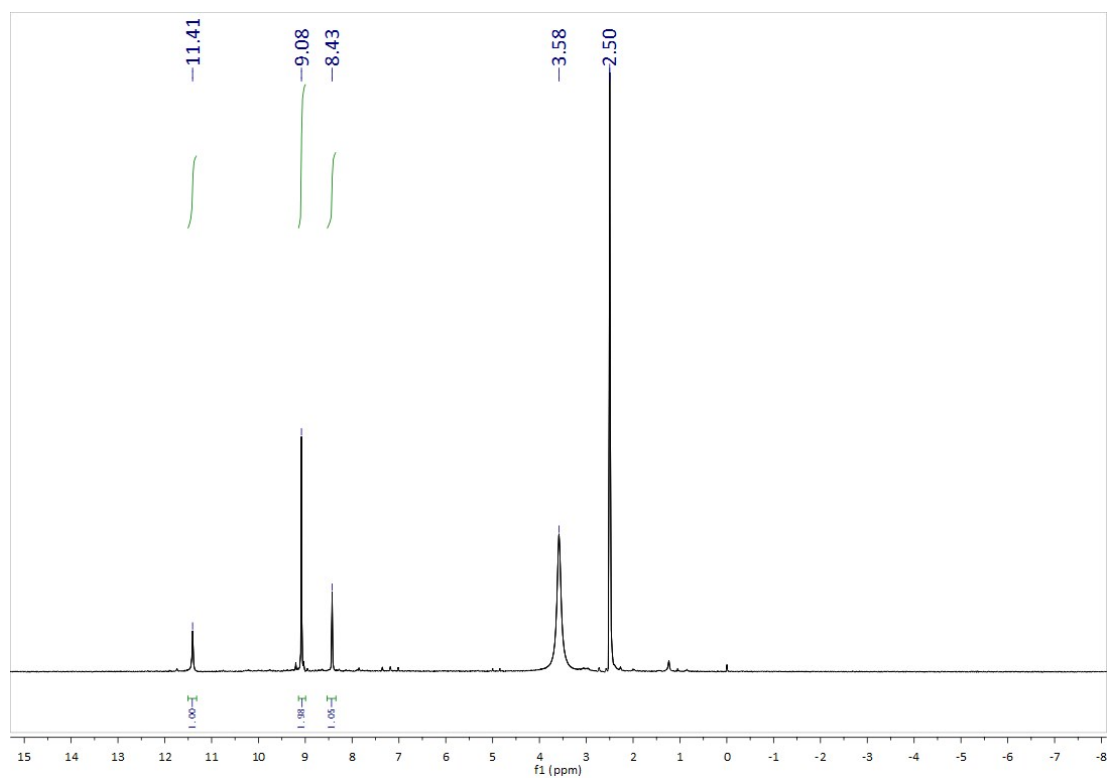


**Figure S16**  $^1\text{H}$  NMR spectra (500 MHz) of **3a** in  $[\text{D}_6]$  DMSO at 25 °C.

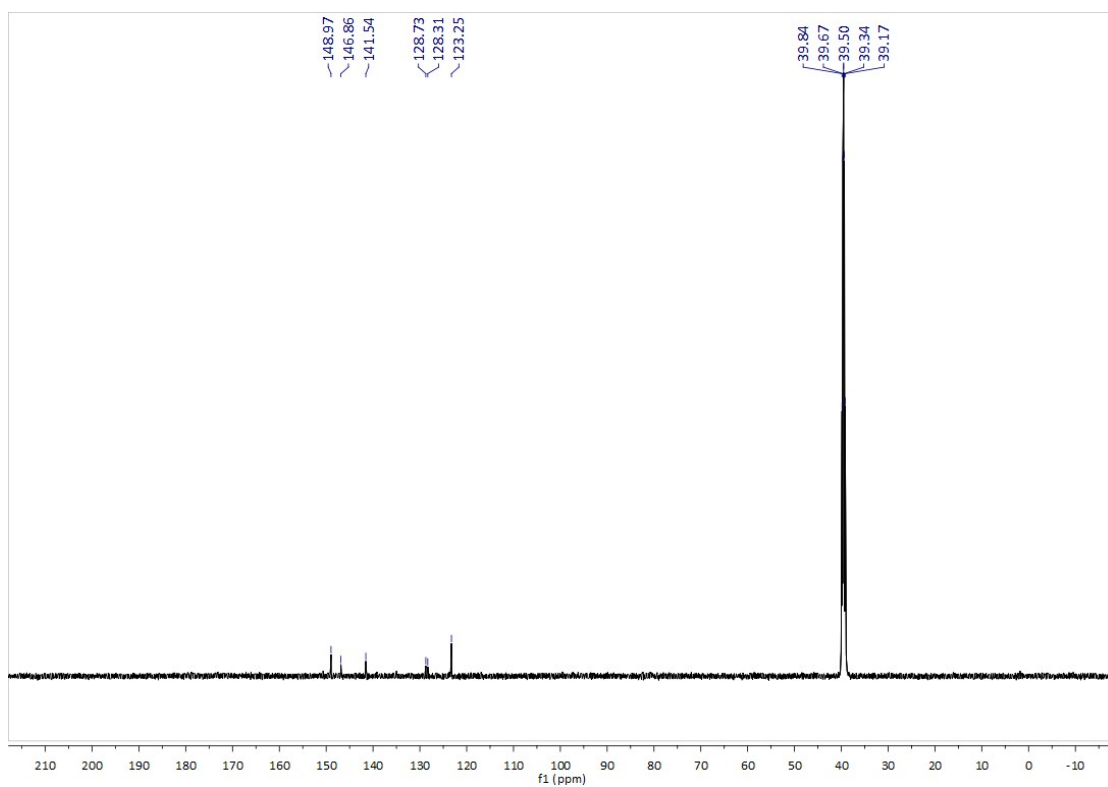


**Figure S17** <sup>13</sup>C NMR spectra (125 MHz) of **3a** in [D<sub>6</sub>] DMSO at 25 °C.

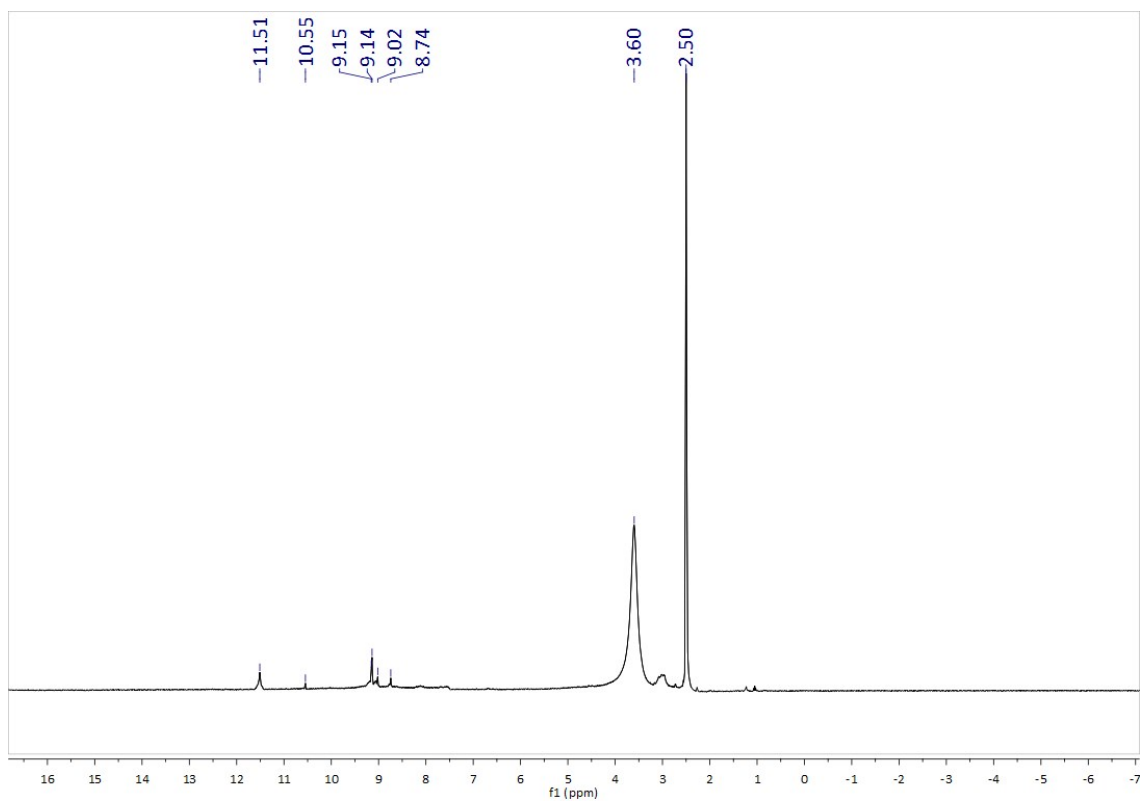


**Figure S18**  $^1\text{H}$  NMR spectra (500 MHz) of **3b** in  $[\text{D}_6]$  DMSO at 25 °C.

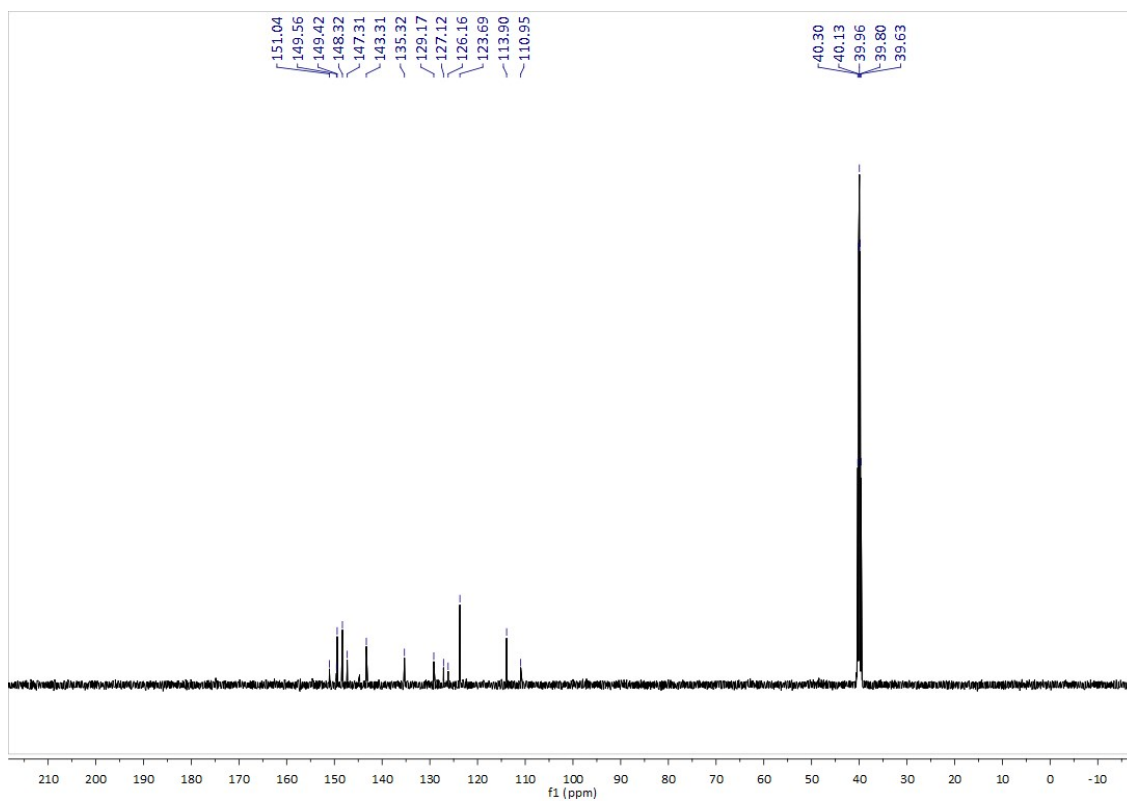


**Figure S19**  $^{13}\text{C}$  NMR spectra (125 MHz) of **3b** in  $[\text{D}_6]$  DMSO at 25 °C.

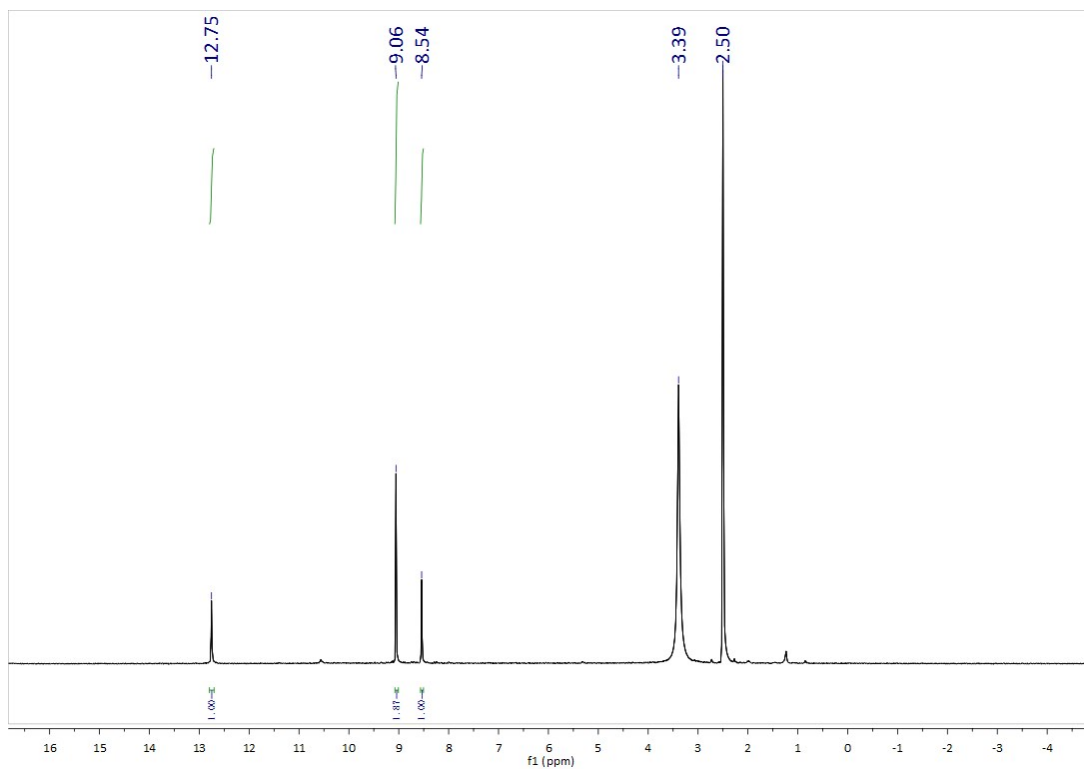


**Figure S20**  $^1\text{H}$  NMR spectra (500 MHz) of **4a** in  $[\text{D}_6]$  DMSO at 25 °C.

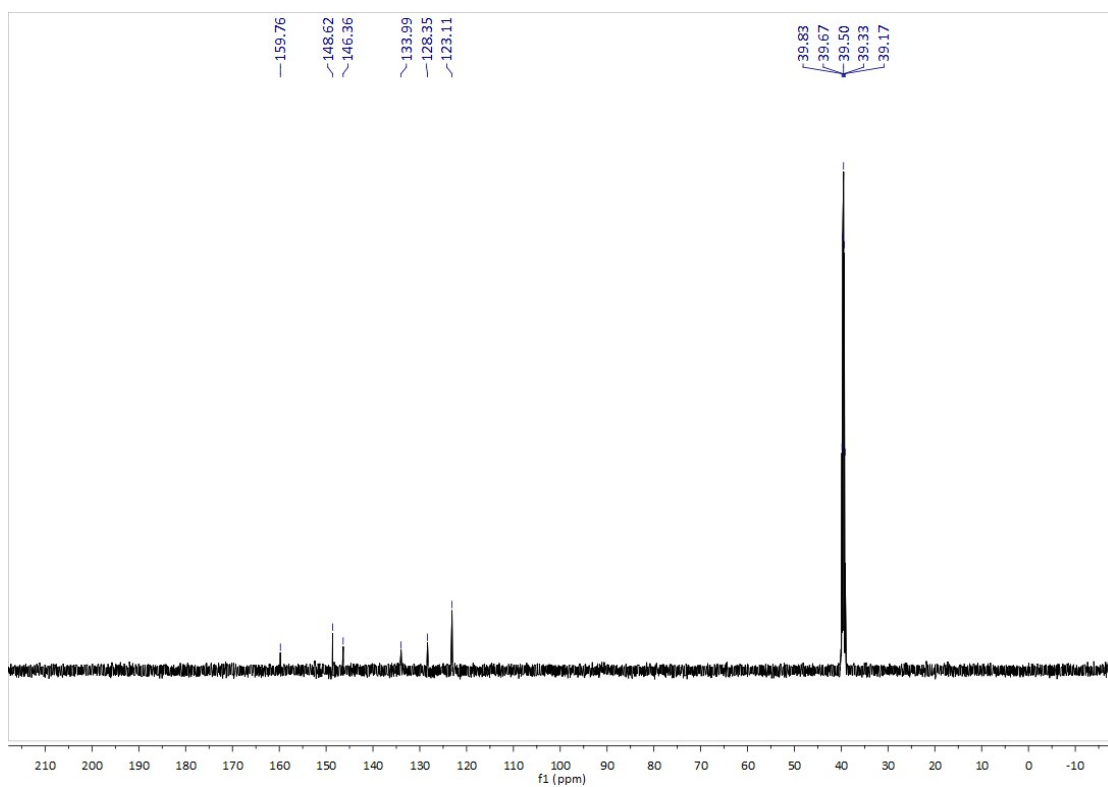


**Figure S21**  $^{13}\text{C}$  NMR spectra (125 MHz) of **4a** in  $[\text{D}_6]$  DMSO at 25 °C.

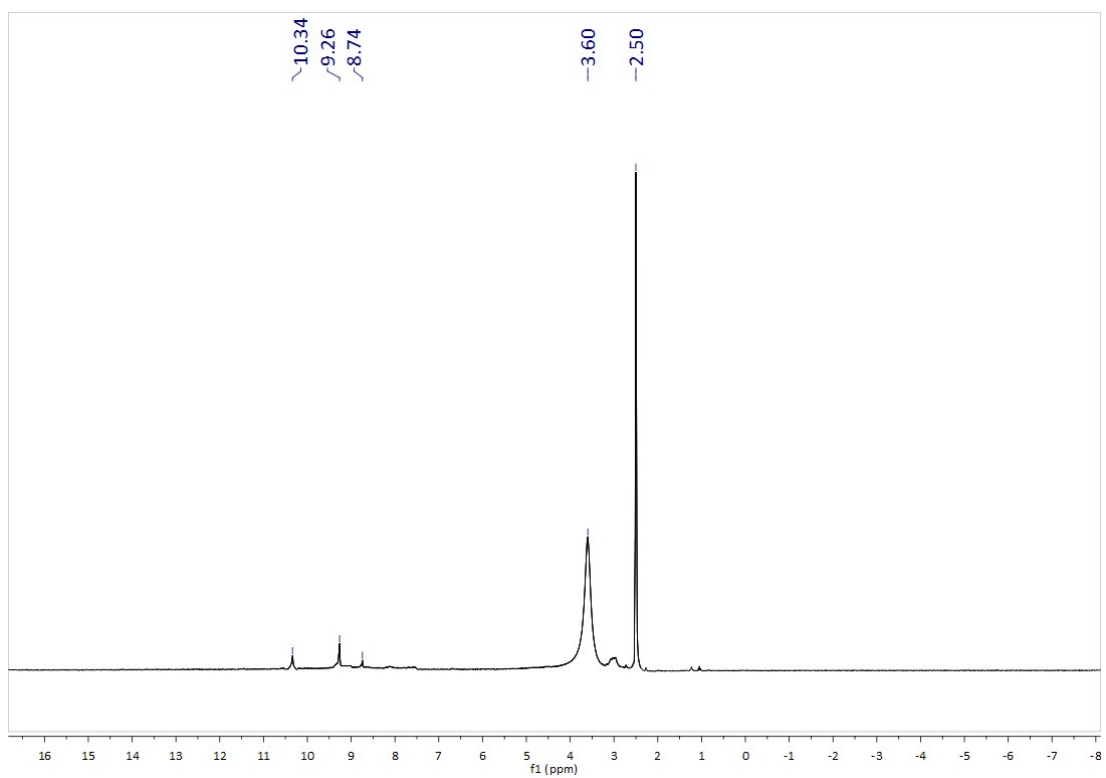


**Figure S22**  $^1\text{H}$  NMR spectra (500 MHz) of **4b** in  $[\text{D}_6]$  DMSO at 25 °C.

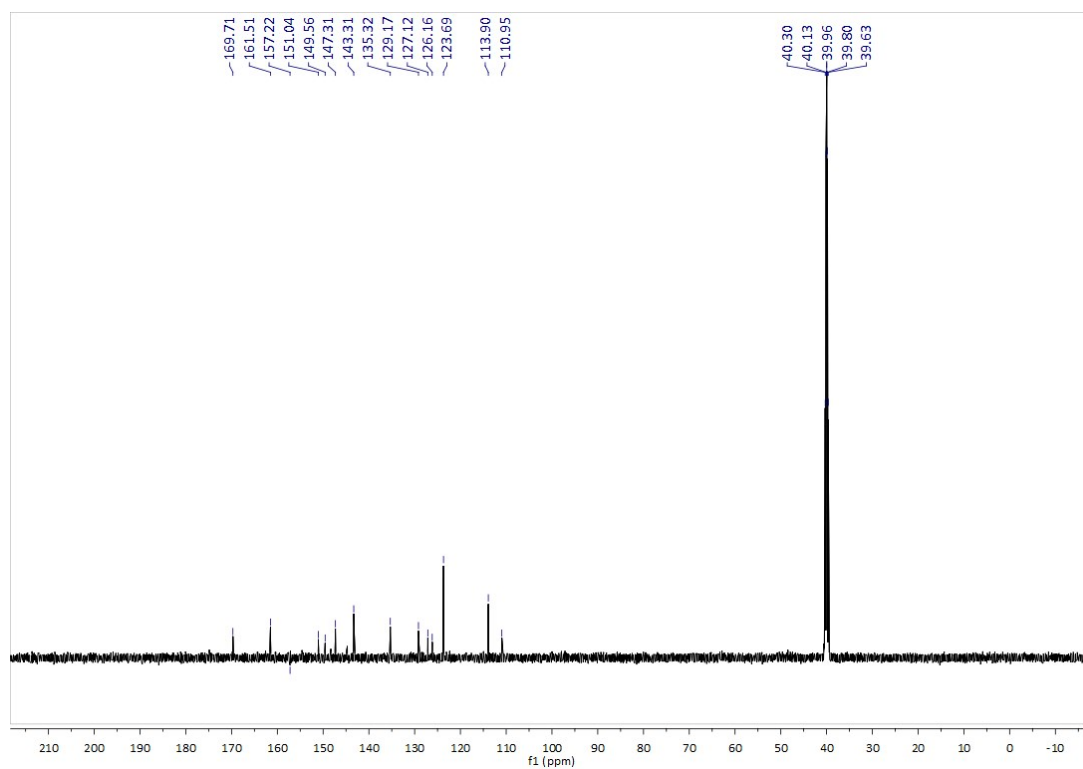


**Figure S23**  $^{13}\text{C}$  NMR spectra (125 MHz) of **4b** in  $[\text{D}_6]$  DMSO at 25 °C.

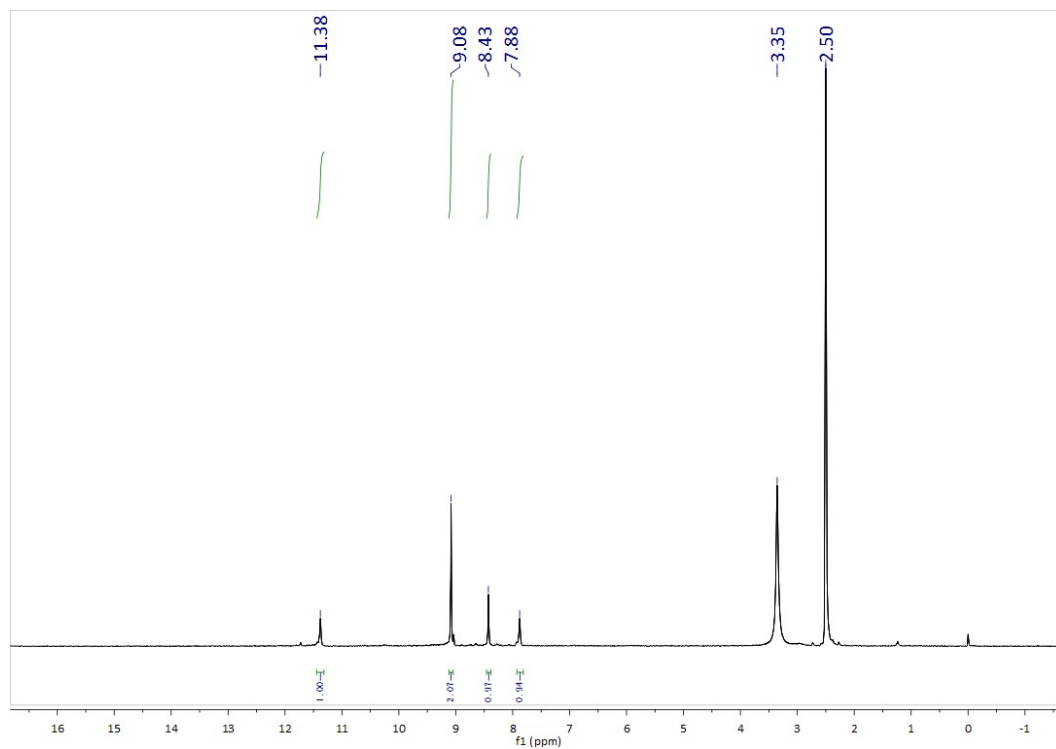


**Figure S24**  $^1\text{H}$  NMR spectra (500 MHz) of **5a** in  $[\text{D}_6]$  DMSO at 25 °C

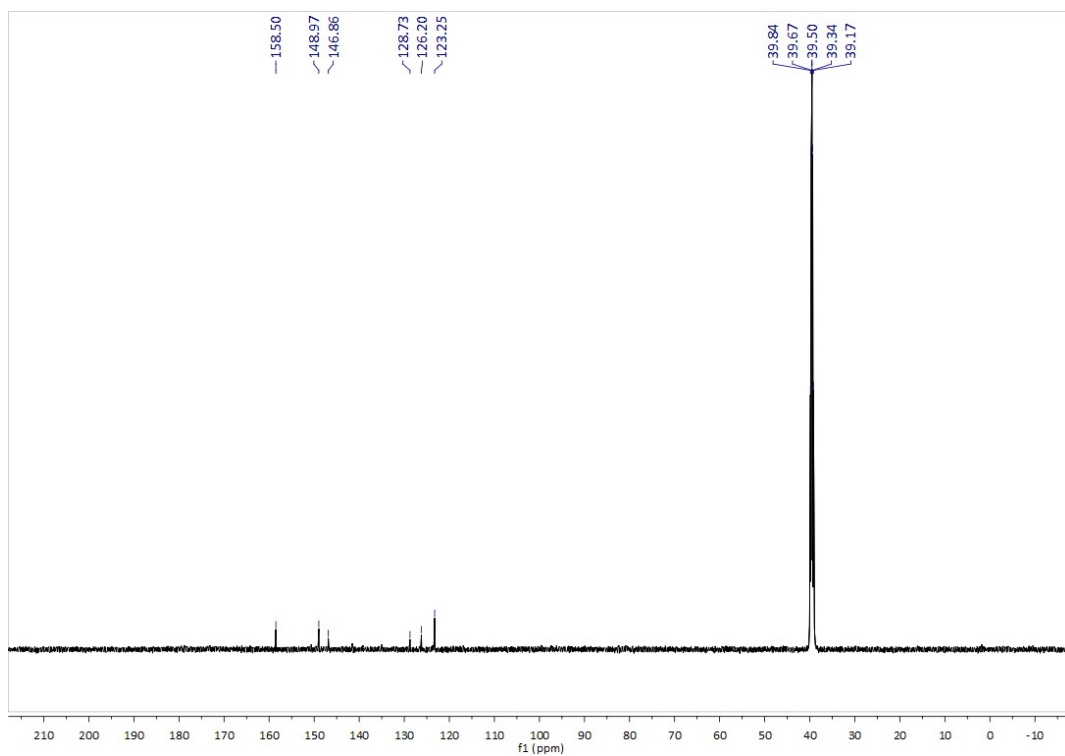


**Figure S25**  $^{13}\text{C}$  NMR spectra (125 MHz) of **5a** in  $[\text{D}_6]$  DMSO at 25 °C

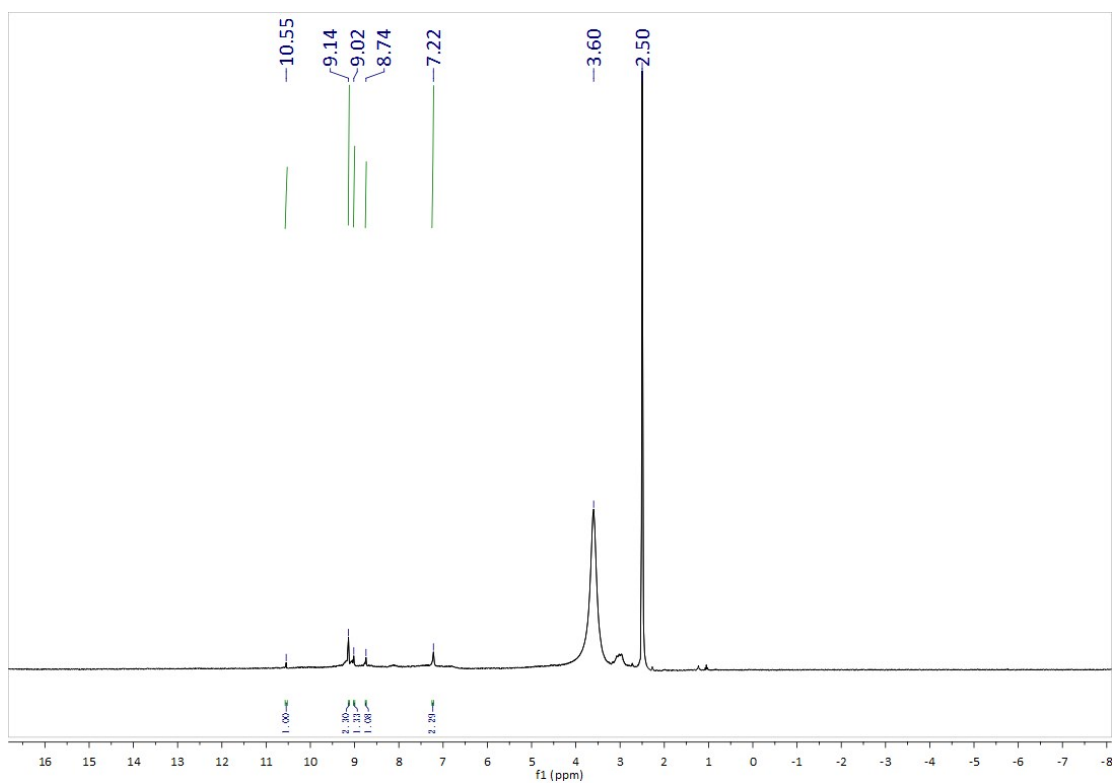


**Figure S26**  $^1\text{H}$  NMR spectra (500 MHz) of **5b** in  $[\text{D}_6]$  DMSO at 25 °C

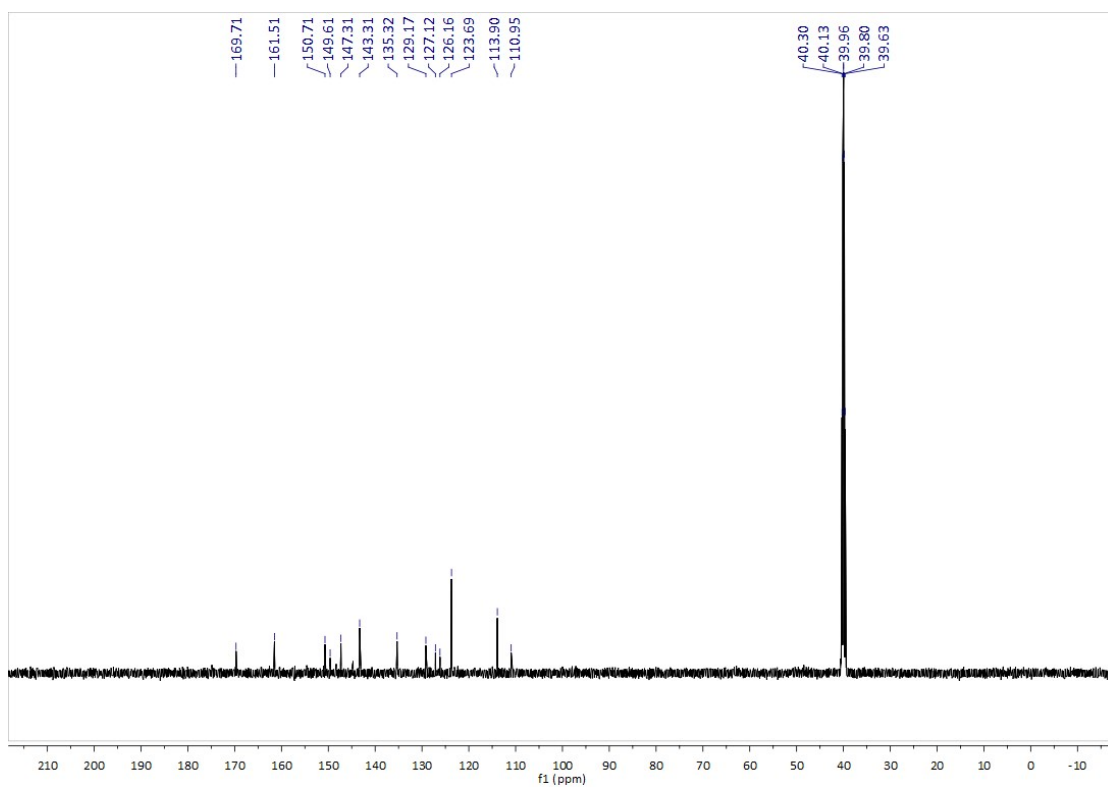


Figure S27  $^{13}\text{C}$  NMR spectra (125 MHz) of **5b** in  $[\text{D}_6]$  DMSO at 25 °C

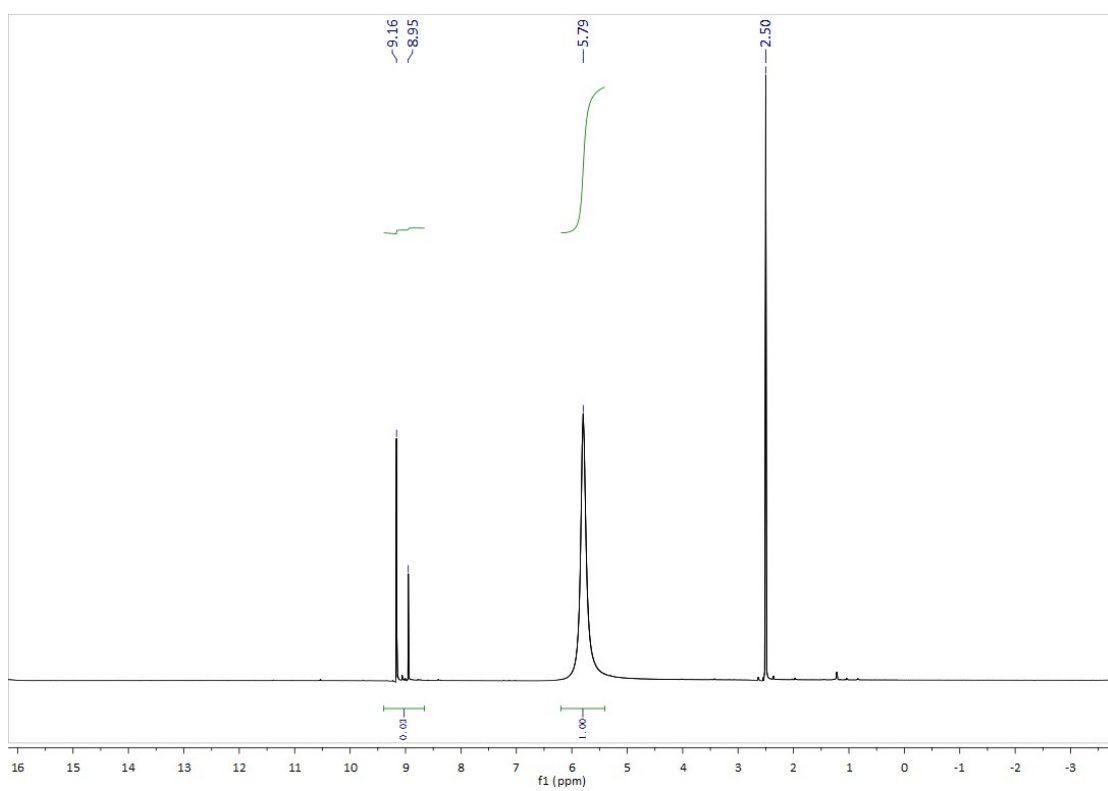
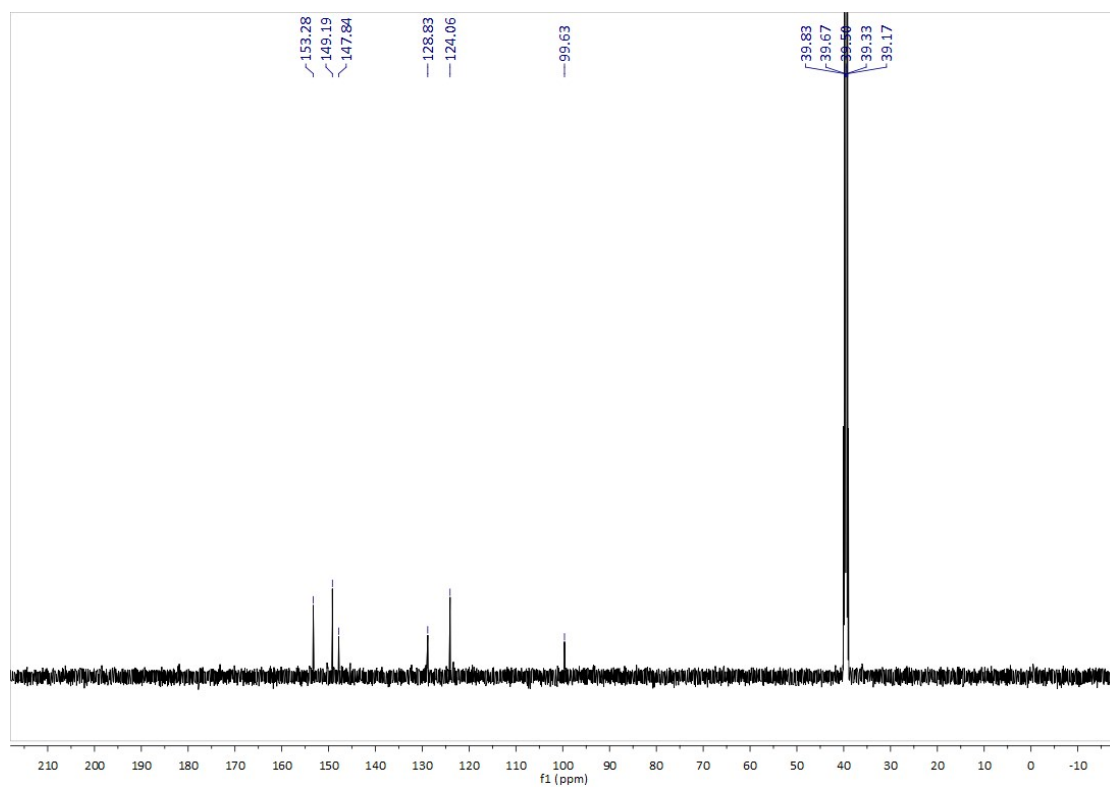
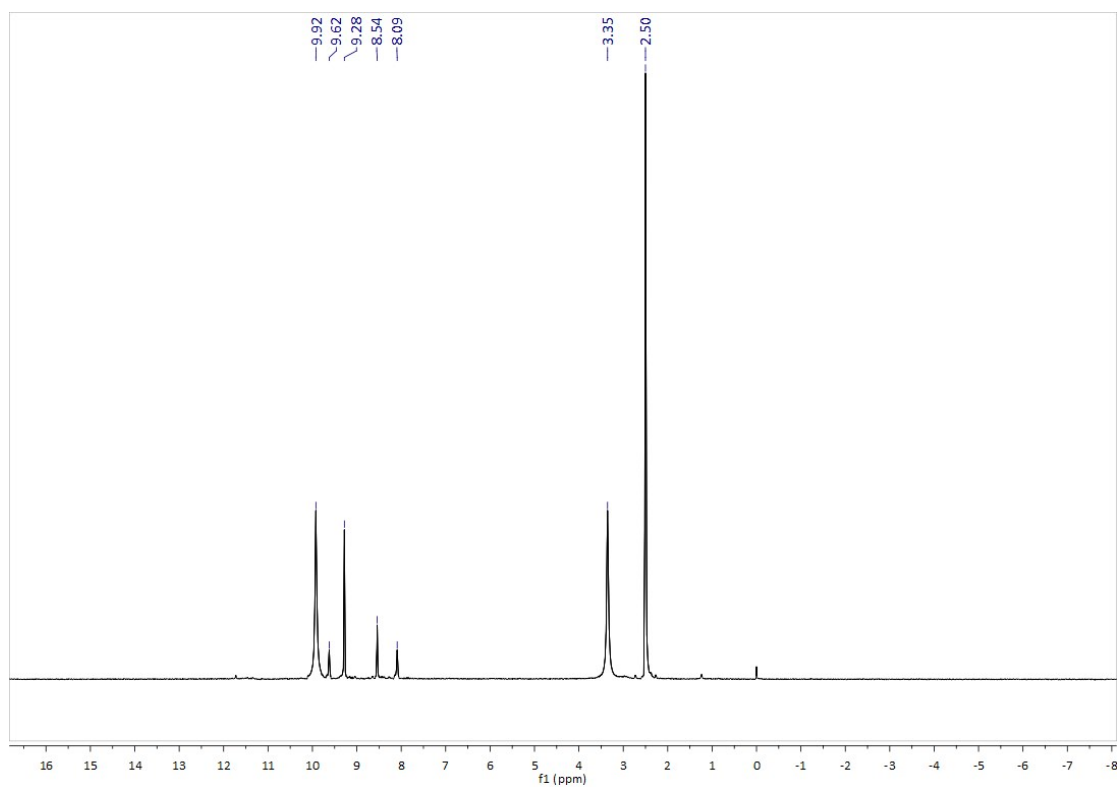


Figure S28  $^1\text{H}$  NMR spectra (500 MHz) of **6a** in  $[\text{D}_6]$  DMSO at 25 °C.



**Figure S29** <sup>13</sup>C NMR spectra (125 MHz) of **6a** in [D<sub>6</sub>] DMSO at 25 °C.



**Figure S30** <sup>1</sup>H NMR spectra (500 MHz) of **6b** in [D<sub>6</sub>] DMSO at 25 °C



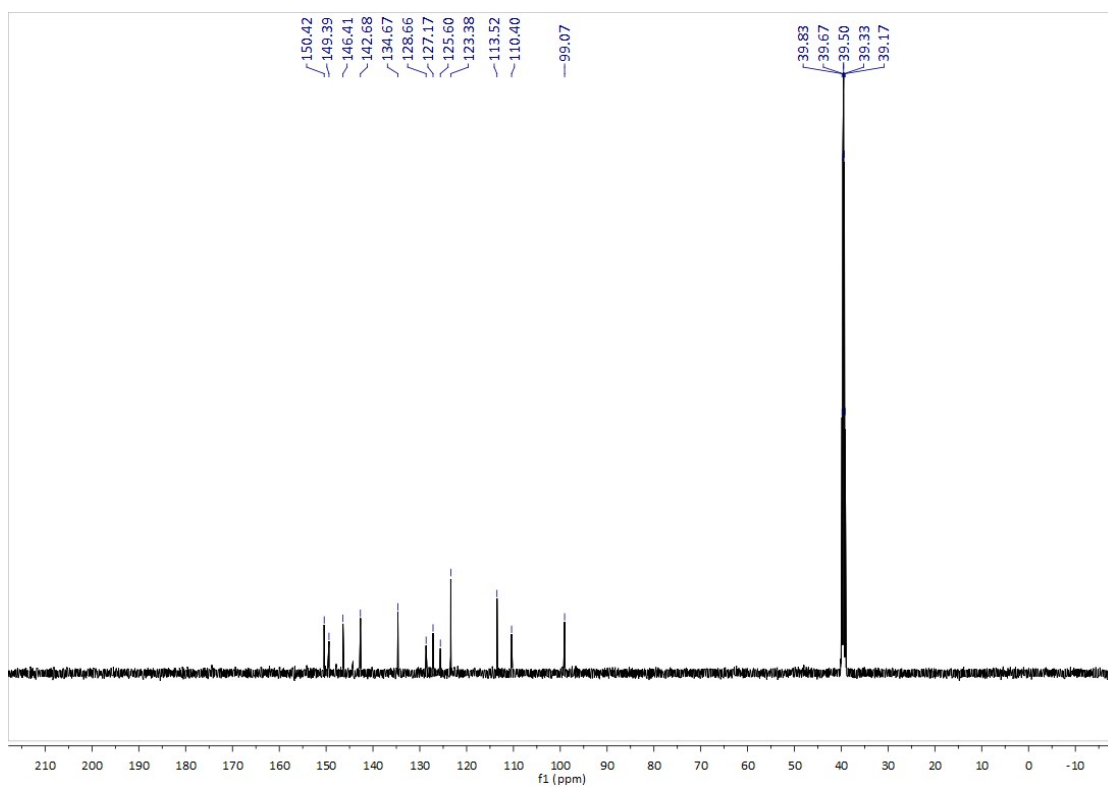


**Figure S31**  $^{13}\text{C}$  NMR spectra (125 MHz) of **6b** in  $[\text{D}_6]$  DMSO at 25 °C

## 7 Mass spectra of compounds

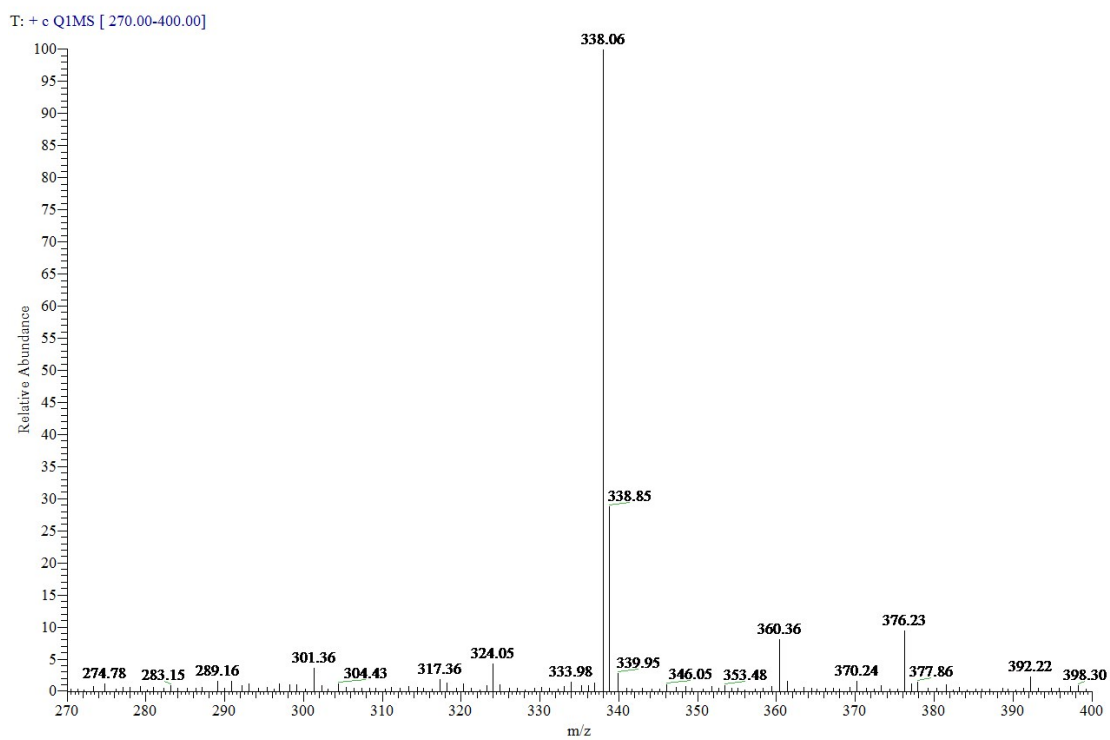


**Figure S32. Mass spectra of compound 1a**

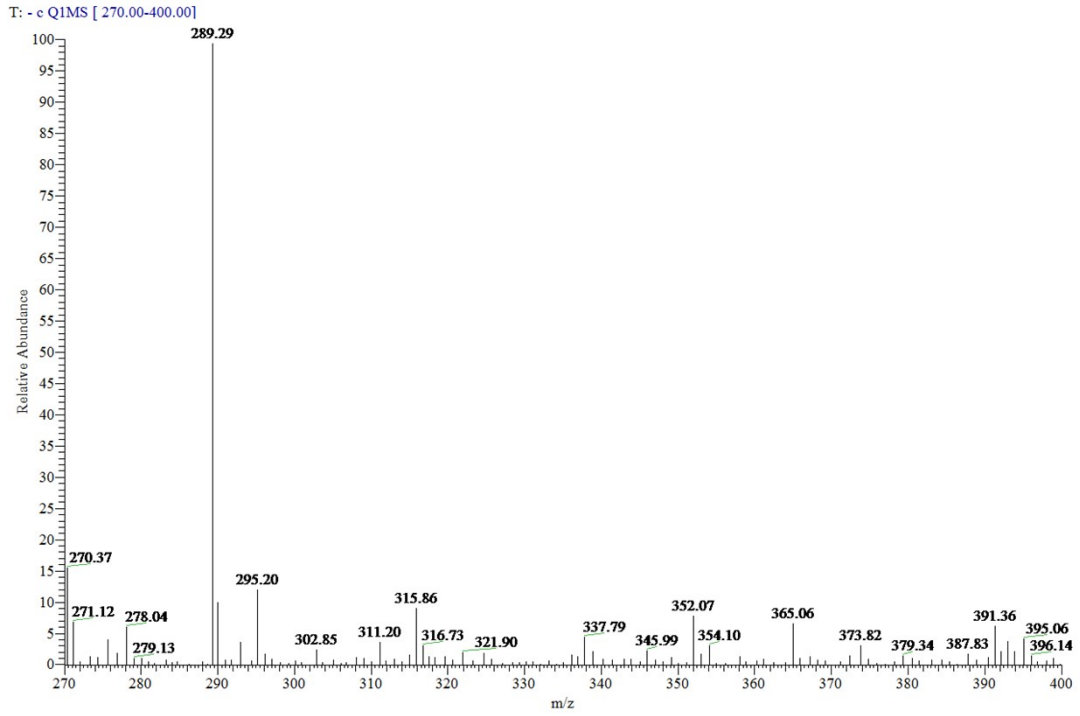


**Figure S33. Mass spectra of compound 1b**

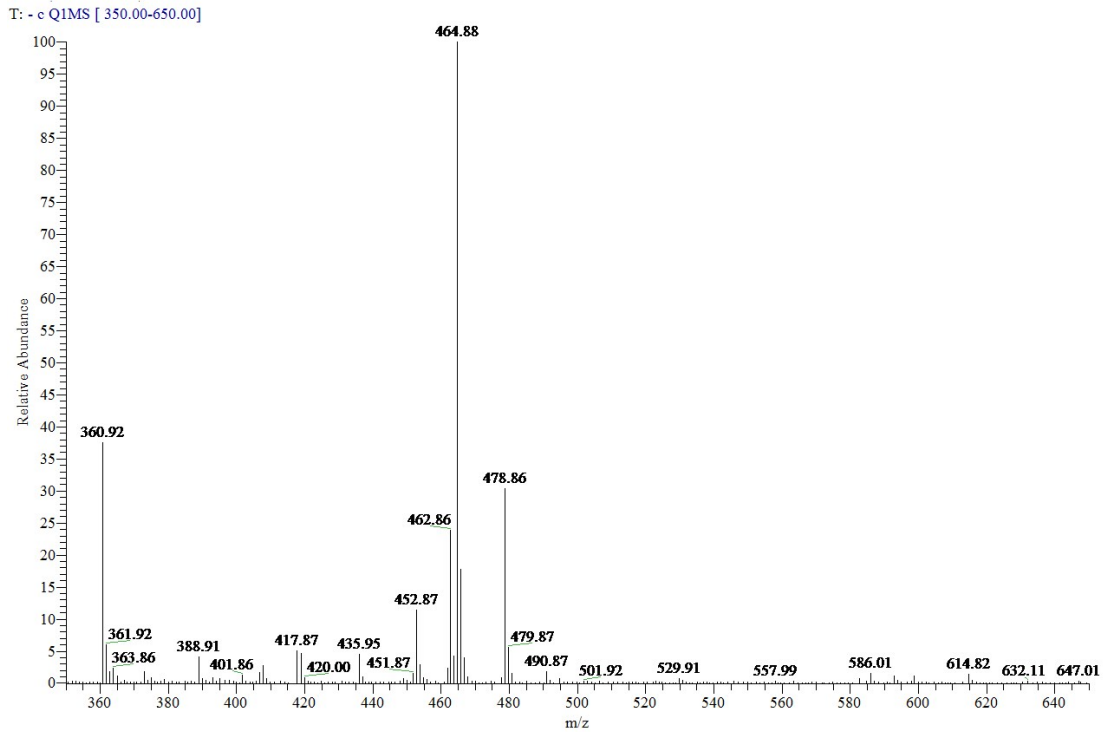


**Figure S34. Mass spectra of compound 2a**

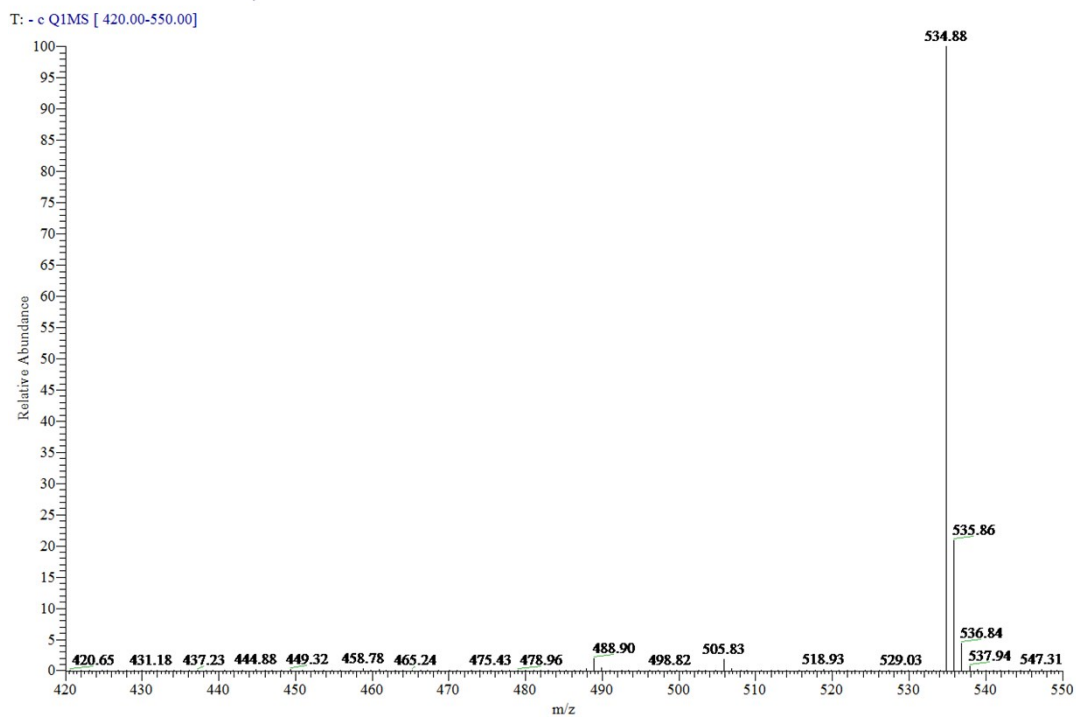


Figure S35. Mass spectra of compound 3a

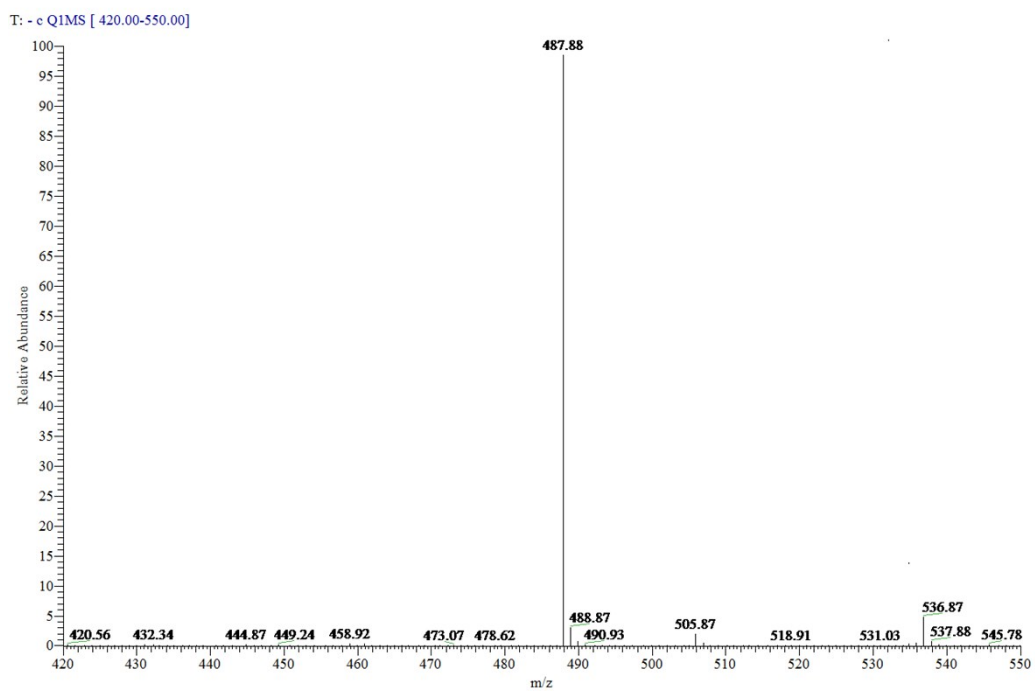


Figure S36. Mass spectra of compound 3b

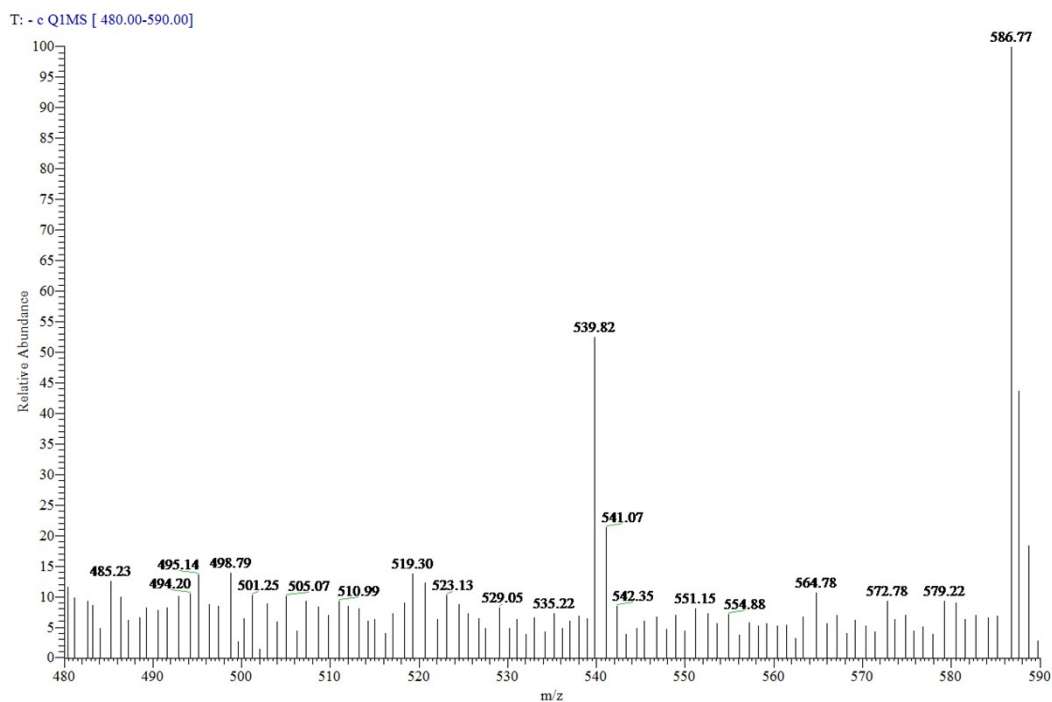
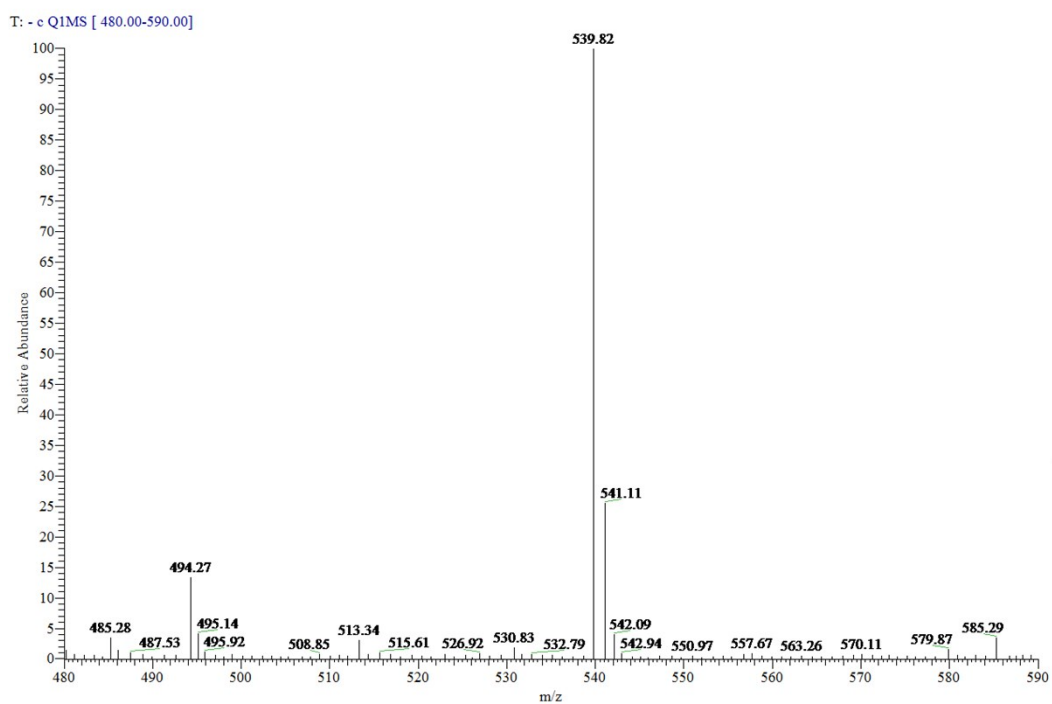
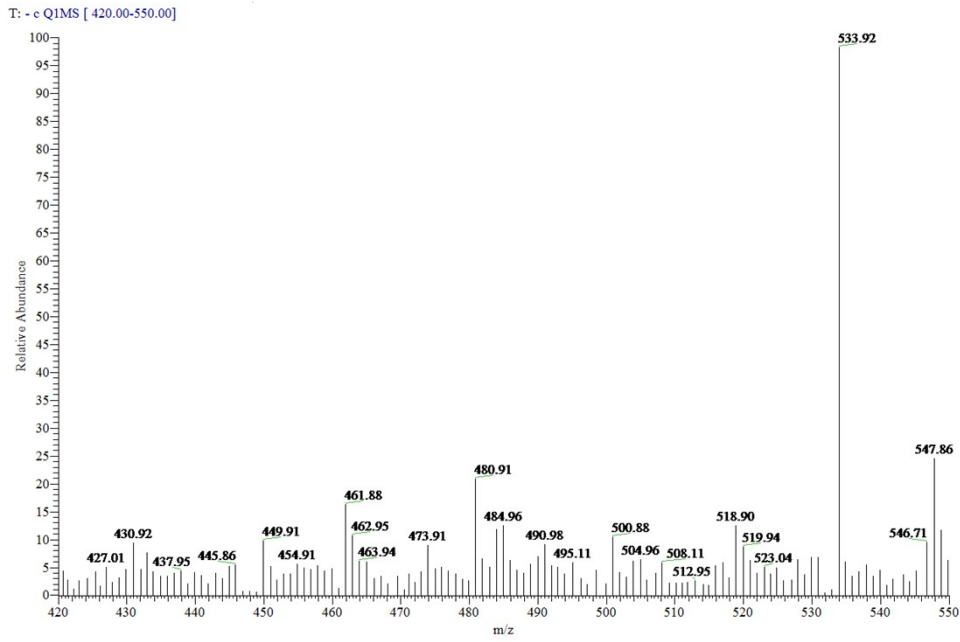


Figure S37. Mass spectra of compound 4a



**Figure S38.** Mass spectra of compound **4b**



**Figure S39.** Mass spectra of compound **5a**

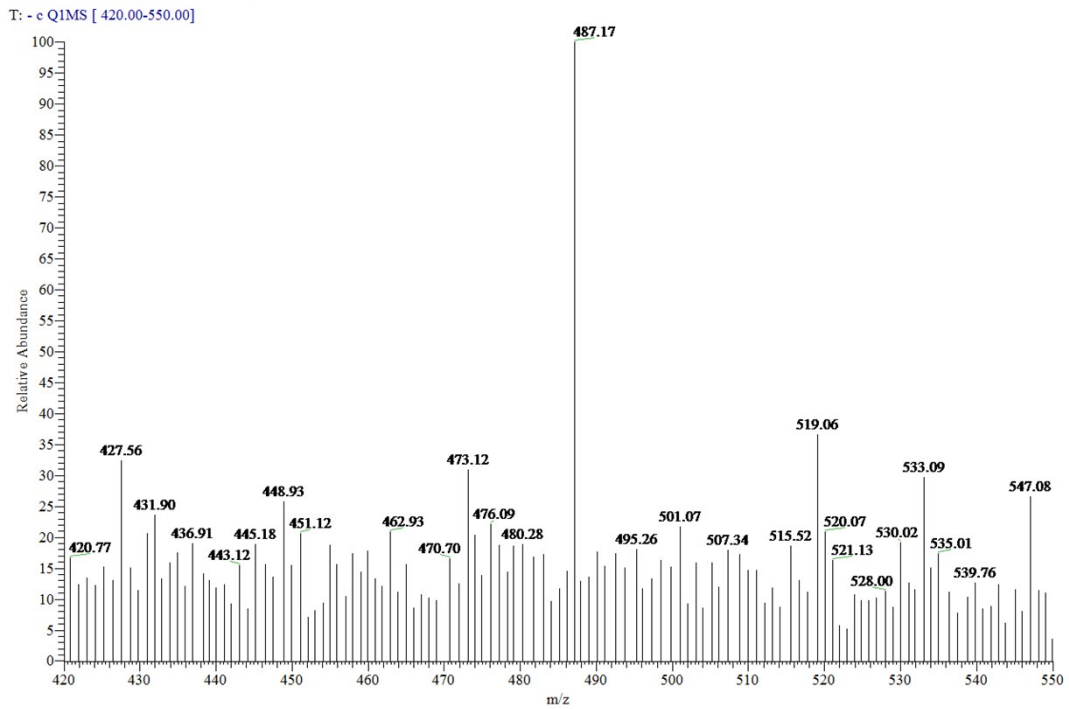


**Figure S40.** Mass spectra of compound **5b**

TJ773\_190523091950 #58 RT: 0.72 AV: 1 NL: 1.49E6  
T: - c Q1MS [ 700.00-850.00]

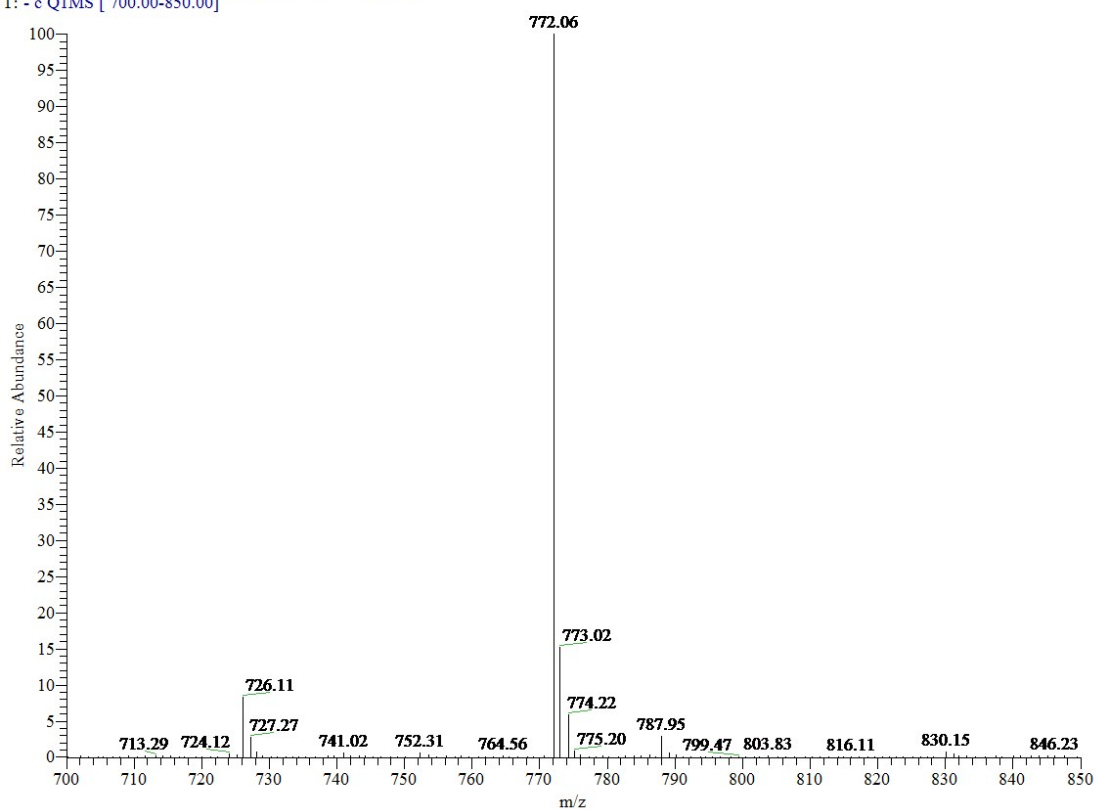
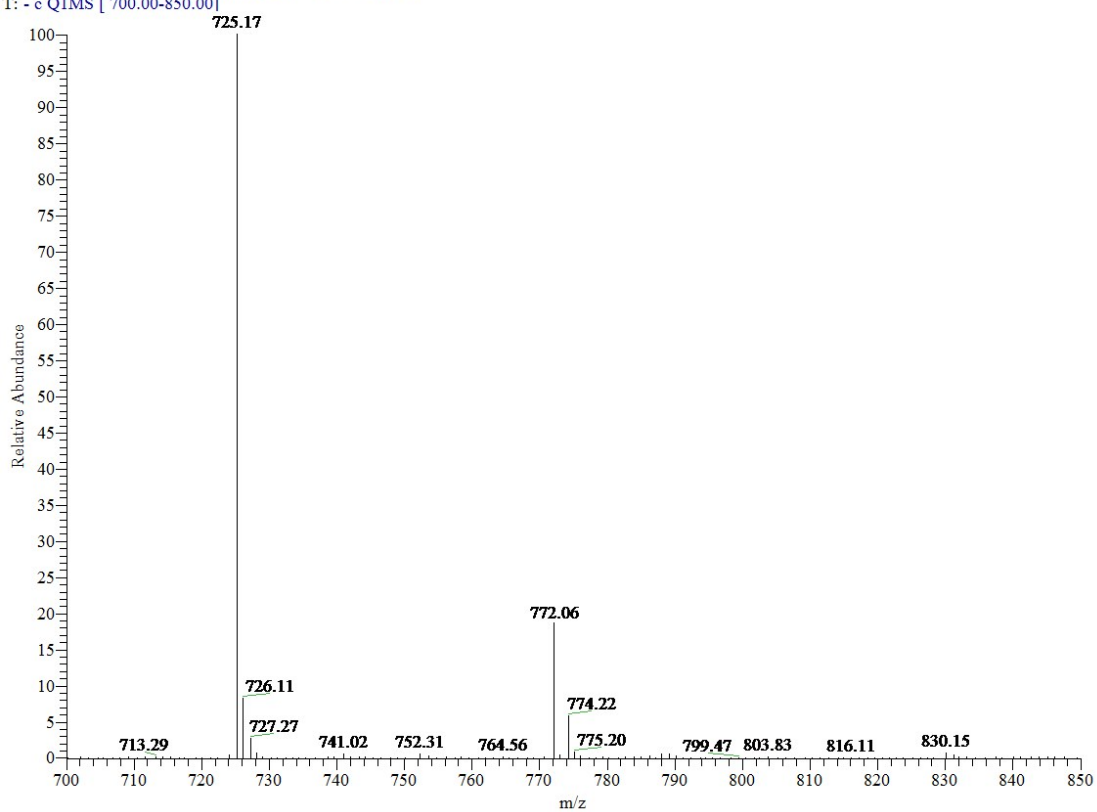


Figure S41. Mass spectra of compound 6a

TJ773\_190523091950 #58 RT: 0.72 AV: 1 NL: 1.49E6  
T: - c Q1MS [ 700.00-850.00]



**Figure S42.** Mass spectra of compound **6b**